APPLICATION OF THE MODIFIED UNIVERSAL SOIL LOSS EQUATION (MUSLE) IN THE PREDICTION OF SEDIMENT YIELD IN AGEWMARIAM EXPERIMENTAL WATERSHED; TEKEZE RIVER BASIN, NORTHERN ETHIOPIA.

M.Sc. THESIS

YONAS REDA SHAREW

JUN. 2022

HAWASSA, ETHIOPIA

APPLICATION OF THE MODIFIED UNIVERSAL SOIL LOSS EQUATION (MUSLE) IN THE PREDICTION OF SEDIMENT YIELD IN AGEWMARIAM EXPERIMENTAL WATERSHED; TEKEZE RIVER BASIN, NORTHERN ETHIOPIA.

YONAS REDA SHAREW

A THESIS SUBMITTED TO THE FACULTY OF BIOSYSTEMS AND WATER RESOURCE ENGINEERING

INSTITUTE OF TECHNOLOGY SCHOOL OF GRADUATE STUDIES

HAWASSA UNIVERSITY

IN PARTIAL FULFILMENT OF THE REQUIREMENTS FOR THE DEGREE OF MASTER SCIENCE IN SOIL AND WATER CONSERVATION ENGINEERING

MAJOR ADVISOR AWDENEGEST MOGES (Ph.D.)

CO-ADVISOR HAILU KINDIE (Ph.D.)

JUN. 2022

HAWASSA, ETHIOPIA

BIOGRAPHICAL SKETCH

The author, Yonas Reda was born in Dec. 1986 to his father Mr. Reda Sharew, and his Mother Mrs. Abebu Taye in Waghimra Zone, Sekota woreda, Sekota town. He attended his elementary education at Medhanialem Elementary school, from 1995 to 2003. He continued his secondary school education at Wagsiyum Admasu Wosen, from 2003 to 2004. Then, he joined Alage ATVET college and graduated with a Diploma in Natural Resources from 2004 to 2007.

After completion of his diploma, he was employed in Sekota woreda agricultural and rural development bureau as a natural resource development agent and worked for three years, and joined back to Wollo University for further study in 2010. He graduated with BSc. Degree in Natural Resource Management in 2012.

Back from school, he served in the Sekota agriculture and rural development bureau as a soil and water conservation expert for about two years. The author then has been employed by Amhara Agricultural Research Institute (ARARI) at Sekota Dry-land Agricultural Research Center starting in June 2015 and served as junior and assistant soil and water conservation researcher in the Soil and Water Management Directorate. He had also served as soil and water management directorate coordinator for more than a year. During this period, he prepared research proposals and carried out experimentation.

After serving for about 4 years in research, he joined the School of Graduate Studies, Hawassa University in 2019 to pursue his Master of Science degree study in Soil and Water Conservation Engineering.

ACKNOWLEDGEMENTS

First, I would like to express my sincere gratitude and respect to my advisors Dr. Awdenegest Moges and Dr. Hailu Kindie. This research would have not been possible without their encouragement, guidance, and advice that enable me to do this M.Sc. thesis research. Thank you for the training and comments you gave me to make this research work completion come true.

Financial support was provided by Sekota Dry-land Agricultural Research Center (SDARC) and Amhara Regional Agricultural Research Institute (ARARI) to cover my research expenses. Thanks.

DEDICATION

This thesis manuscript is dedicated to my family.

STATEMENT OF THE AUTHOR

First, I declared that this thesis is my original work and all sources of materials used for this thesis have been duly acknowledged. This thesis has been submitted in partial fulfillment of the requirements for an M.Sc. degree in Soil and Water Conservation Engineering at Hawassa University and is deposited at the University Library to be made available to borrowers under the rules of the library. I solemnly declare that this thesis is not submitted to any other institution anywhere for the award of any academic degree, diploma or certificate. A brief quotation from this thesis is allowable without special permission provided that accurate acknowledgment of the source is made.

Name Yonas Reda Sharew Signature……

Place: Hawassa University

Date of submission……

E-mail address: yonashimra@gmail.com

ABBREVIATIONS AND ACRONYMS

AMC I	*Antecedent Moisture Condition I*
AMC II	*Antecedent Moisture Condition II*
AMC III	*Antecedent Moisture Condition III*
ARI	*Average Recurrence Interval*
C	*Cover and Management factor*
CN	*Curve number*
DEM	*Digital Elevation Model*
ESRI	*Environmental Systems Research Institute*
FAO	*Food and Agricultural Organization*
GIS	*Geographic Information System*
GPS	*Global Positioning System*
HRU	*Hydrological Response Unit*
HSG	*Hydrologic soil group*
IDF	*Intensity Duration Frequency*
IDW	*Inverse Distance Weighting*
K	*Soil Erodibility factor*
KML	*Keyhole Markup Language*
L	*Slope Length factor*
MUSLE	*Modified Universal Soil Loss Equation*
NRCS	*Natural Resources Conservation Service*
NMA	*National Meteorology Agency*
P	*Support Practice Factor*

RUSLE	*Revised Universal Soil Loss Equation*
S	*Slope Steepness factor*
SCS	*Soil Conservation Service*
SLEMSA	*Soil Loss Estimation Model for Southern Africa*
SWAT	*Soil and Water Assessment Tool*
SWC	*Soil and Water Conservation*
USDA	*United States Department of Agriculture*
USGS	*US Geological Survey*
USLE	*Universal Soil Loss Equation*
WMO	*World Meteorological Organization*
WS	*Watershed*
λ	*Initial Abstraction to Storage ratio*

TABLE OF CONTENTS

LIST OF TABLES

LIST OF FIGURES

LIST OF APPENDIX TABLE

LIST OF APPENDIX FIGURES

ABSTRACT

The severe effect of soil and water resource degradation in Ethiopia is putting pressure to take soil and water erosion control measures. To support the planning, management, and appropriate use of the soil and water resources the Modified Universal Soil Loss Equation (MUSLE) was used to model eventual sediment loss in Agewmariam experimental watershed. The model uses different methods for the estimation of the runoff energy, soil erodibility, slope length & steepness, cover management, and support practice factors input parameter values; so that calibration, evaluation, and validation of parameter values become mandatory. The model input parameters were collected from a combined process of field observation, laboratory analysis, Google Earth Pro, and GIS processing while cover management and support practice are adopted from literature. Analysis of input parameters was done with the help of ArcGIS and MS-EXCEL. The input parameter maps were overlaid to assign a value and the combined effect of the parameters for the suspended sediment yield was calculated on a raster calculator. The runoff energy factor is the most sensitive parameter followed by the slope length and steepness factor. For the calibration period, the event-based mean observed and estimated suspended sediment yields were 0.2 and 0.23 ton/ha respectively with a little overestimation; while for the validation period, is 0.7 and 0.53 ton/ha with great underestimation. The model evaluation shows a 0.85 coefficient of determination, a 0.85 coefficient of efficiency, and an index of agreement value of 0.96 for the calibration period which can be considered a good model performance, whereas a 0.84 coefficient of determination, 0.65 coefficient of efficiency, and an index of agreement value of 0.83 for the validation period. The result revealed the use of the MUSLE model in its original form without calibration is not proper. The evaluation result shows the model with the appropriate calibration is a good estimator of sediment yield so that it can be used for spatial prioritization of soil and water conservation need within the watershed or extrapolated to the neighboring similar watersheds.

Keywords: MUSLE, Sediment yield, Rating Curve, Curve Number, Agewmariam WS.

1 INTRODUCTION

1.1 Background

The management, conservation, and use of soil and water resources are critical to human well-being and more important now than ever before to meet the high demands for food production and satisfy the needs of an increasing world population (Humberto and Rattan, 2008). It has also been indicated that nowhere is the severe effect of poverty and environmental degradation more evident than in Ethiopia (Mekonen and Tesfahunegn, 2011).

Soil erosion by water continues to be a serious problem throughout the world (Flanagan *et al.*, 2002) and it is indicated by Hurni *et al.*, (2016) that Soil erosion is the most dangerous ecological process observed in Ethiopia, degrading precious soil resources that are the basis for agricultural production and food for the people and which provide many other ecosystem services.

In Ethiopia, out of the estimated 60 million ha of agriculturally productive areas, nearly 27 million ha experience erosion, 14 million ha are considered eroded and require rehabilitation, and 2 million ha are considered lost with an estimated total loss of 2 million m^3 of topsoil per year and with an average annual soil loss from cultivated lands of 100 t ha^{-1}(Mekonen and Tesfahunegn, 2011). Soil erosion occurs mainly during the rainy season in the form of water erosion. Rills, gullies, and brown rivers full of sediment show that a lot of soil is carried away and lost for agricultural production (Hurni *et al.*, 2016).

The development of improved soil erosion prediction technology is required to provide policymakers, conservationists, farmers, and other land users with the tools they need to assess the current status of the land resource and the potential need for enhanced or new policies to protect soil and water resources and to examine the impact of various management strategies on soil loss and sediment yield and plan for the optimal use of the land (Flanagan *et al.*, 2002).

Erosion prediction is most needed by conservationists at the field level who work directly with farmers and other land users, which has large implications for the development and adoption of this technology (Flanagan *et al.*, 2002). The term 'erosion modeling' is used to indicate the total detachment of soil particles by rainfall and runoff in an area, but also to predict the soil loss from a specific area. In a wider context it is used to indicate the hazard or risk associated with the removal of topsoil, both onsite (fertility loss, gullying) and offsite (muddy floods and downstream pollution) (Jetten and Maneta, 2011).

Modeling water and wind erosions are important to understand the processes governing soil erosion, predicting runoff and soil erosion rates, and identifying or choosing appropriate measures of erosion control. Modeling permits: (1) understanding of the driving processes, (2) evaluation of on-site and off-site impacts on soil productivity and water and air pollution on large scale, (3) identification of strategies for erosion control, and (4) assessment of the performance of soil conservation practices for reducing water and wind erosion. Well-developed and properly calibrated models provide good estimates of soil erosion risks (Humberto and Rattan, 2008).

The most widely used empirical soil erosion models include Universal Soil Loss Equation (USLE), Revised Universal Soil Loss Equation (RUSLE), Modified Universal Soil Loss Equation (MUSLE), and Soil Loss Estimation Model for Southern Africa (SLEMSA) (Alemayehu *et al.*, 2019). Although USLE, RUSLE, and MUSLE have had practical success as an aid in conservation management decisions and the reduction of soil erosion from agricultural lands, they are not capable of simulating soil erosion as a dynamic process distributed throughout a watershed and changing over time. Although the MUSLE can estimate soil loss from a single event, neither it nor the USLE nor the RUSLE can estimate detachment, entrainment, transport, deposition, and redistribution of sediment within the watershed and are of limited application (Randle *et al*., 2006).

The MUSLE is a modified form of USLE. While USLE predicts sediment yield based on rainfall, MUSLE predicts it by using the runoff factor, which accounts for the antecedent soil water content. This modification allows the use of USLE to predict sediment loss on a storm event basis (Humberto

and Rattan, 2008). Currently, only the MUSLE model is applied in storm-wise sediment yield prediction. This is due to a lack of adequate data regarding rainfall, channel geometry, and hydraulics of entire stream systems which would otherwise be required. The MUSLE model optimizes hydrologic model parameters to estimate sediment yield (Sadeghi *et al.*, 2007).

The event-based prediction provides a cumulative improvement in the planning and implementation of soil and water conservation. In general, this study allows leveraging the model in the practical use for soil and water resource conservation and management process.

1.2 Statement of the problem

A major requirement in watershed management is the establishment of soil and water conservation technologies. Many of these have existed for a long time, but information to support the selection of those that are appropriate for ecological and socioeconomic conditions has not been readily available to farmers and field officers (Namirembe *et al*, 2015).

While there is an increased risk of soil degradation when land is put under cultivation, rural societies do their best to gradually build up techniques that will allow the long-term preservation of soil productivity. However, when new needs emerge too fast, a crisis will arise that rural society cannot respond to in time and here the state must step in to help overcome the crisis with technical assistance and financial support (Roose, 1996).

Surely, the only way to effectively deal with a problem in a given catchment or at a given field site is to undertake detailed field observations and measurements of erosion and its controlling factors at that site and, based on an analysis of the results, to select appropriate measures to control the problem. Unfortunately, such detailed field measurements are often very costly and must be carried out over many years, probably ten or more, to collect representative data. In contrast, many problems must be addressed immediately and cannot

wait for a solution some years later by which time considerable environmental damage may have occurred (Nearing, 2011).

Accurate prediction of sediment yield from watersheds is important from land use, management, and environmental standpoints. Sediment yield models that require runoff input can be attached to hydrologic models to predict daily sediment yield (Williams and Berndt, 1977). By understanding how model developers operate and following a common methodology, users will be better equipped to decide what questions need to be asked when selecting a model to meet their specific objectives (Nearing, 2011).

MUSLE increases sediment yield prediction accuracy eliminates the need for delivery ratio, and applies to individual storms (Williams and Berndt, 1977). The predicting ability of MUSLE to storm event-based soil loss enables the planners to emphasize the high spatial and temporal variability of eventual conditions in the area for its cumulative improvement in planning and implementation of soil and water conservation.

1.3 Significance of the study

Soil erosion modeling helps to provide information about soil erosion processes that helps effective planning and decision making to implement management interventions, such as watershed-based soil and water conservation and resource management. On the other hand, the study watershed Agewmariam is a small-sized watershed established as a representative watershed to the Wag and Lasta areas to provide representative experimental results. High investment costs are incurred on the watershed to meet the watershed development plan in the area. Therefore, calibrating and validating the soil erosion model helps to make accurate and precise inferences and extrapolations to the entire area of interest from the experimental data of the watershed.

1.4 Objectives of the study

1.4.1 General objective

To Improve the sediment yield prediction accuracy of the Modified Universal Soil Loss Equation (MUSLE) for the local condition using hydrosedimentological data from Agewmariam experimental model watershed for its use as a tool for planning soil and water conservation and watershed management.

1.4.2 Specific objectives

- To estimate storm event sediment yield in Agewmariam watershed using Modified Universal Soil Loss Equation (MUSLE).
- To assess the sediment yield prediction accuracy of Modified Universal Soil Loss Equation (MUSLE).

1.5 Research questions

- How much sediment is lost in the study watershed within an individual storm?
- Does the MUSLE model simulate event-based sediment yields well?
- What are the most influential model parameters?
- How to calibrate and validate MUSLE for the local condition?

2 LITERATURE REVIEW

2.1 Soil erosion and control efforts in Ethiopia

Ethiopia has mainly complex and fragile landscapes; In consequence land degradation seriously affects the livelihoods and food security of millions and threatens the livelihood of many more. Consequently, the agricultural system of the country is progressively impoverished and more vulnerable to shocks. These are serious constraints to sustainable development and the main cause of unstable, over-simplified & drought-prone production systems (Desta *et al.*, 2005). In Ethiopia, land degradation, low and declining agricultural productivity, and poverty are severe and interrelated problems that appear to feed off each other (Yesuf *et al.*, 2005).

Increased pressure on land use of the hill slopes since the 1970s has resulted in degradation in the highlands of Ethiopia where agriculture is based on small-scale cereal production (Desta *et al.*, 2009).

Soil erosion is one facet of land degradation that affects the physical and chemical properties of soils (Esser *et al.*, 2002). The main land degradation arises from high soil erosion rates as a result of steep slopes, continuous encroachment, and cultivation of marginal lands; long history of deforestation, overgrazing, negative coping strategies such as the burning of animal dung, extensive use of charcoal, reduced rotation periods, and others; Recurrent cycles of drought and inadequate infrastructure have further aggravated the problem (Desta *et al.*, 2005).

However, soil erosion is widely perceived to be a major problem, particularly in the highlands of Ethiopia, which is considered a direct result of past agricultural practice in the

highlands due to dissected terrain, intense rainfall, and growing human and animal population leading to accelerated erosion (Badege, 2001).

The amount of soil loss on cultivated lands ranges from 1 t/ha/yr. to more than 300 t / ha/year and as Hurni *et al.,* (2010) reported an average of approximately 40 t / ha/year of soil loss was measured on cultivated land through a plot experiment. Nationwide, the annual rate of soil loss (more than 1.5 billion tons) is much higher than the annual rate of soil formation with an estimated cost of close to one billion Ethiopian birrs each year (Gelagay and Minale, 2016).

Soil loss in the highlands of Ethiopia was estimated to be about 200–300 t / ha/year (Gelagay and Minale, 2016), (Amsalu and Mengaw, 2014). Muche *et al.*, (2013) reported according to FAO, (1986), 50% of the highlands of Ethiopia are already significantly eroded and caused a decline in land productivity at the rate of 2.2% per year. Soil erosion is severe on cultivated lands. Appropriate physical conservation measures are not adequately introduced and practiced by the farmers (FEPA, 2004).

In light of the increasing population (2.2 percent growth per annum) and the low levels of urbanization (only 16 percent of the population live in urban areas), all projections indicate that land degradation in Ethiopia is bound to proceed at aggravated rates unless significant progress is made in conservation, rehabilitation, and restoration (Yesuf *et al.*, 2005).

Since Ethiopia has a great climatic variety, from dry to wet, and also many different altitudes, from lowlands to highlands, the same conservation technologies cannot be applied everywhere. Therefore, it is necessary to know the characteristics of an area where soil and water conservation is to be implemented. Cultivated land requires conservation measures

different from those required on grassland. Forests, in turn, require other measures (Hurni *et al.*, 2016).

A massive effort is being made in soil conservation by the Ministry of Agriculture. The Community Forest and Conservation Development Department has already implemented soil conservation measures on more than 1 million hectares in the last ten years (Grunder, 1988), (Adimassu et al., 2018). Several projects involving significant financial investment have been implemented to reverse land degradation and improve land productivity in Ethiopia since the 1970s (Adimassu et al., 2018).

There is also an effort to prepare a guideline book to make it easy for users to determine the agroecological zone of the work area to find the selection of conservation measures, recommendations for the different agroecological zones, and a description for each recommended conservation measure with drawings (Hurni, *et al*., 2016).

There are soil and water conservation structures and other management measures recommended for Ethiopian conditions as listed in (Hurni, et al., 2016), (Desta, et al., 2005). Adimassu et al., (2018) categorized the soil and water conservation practices implemented under farmland management, hillside management, and gully rehabilitation practices, including check dams and cut-off drains. Works of literature show that among the soil and water conservation practices in Ethiopia, fanyajuu occupies 2-15% of the land area for a slope of 3-15%, stone bunds occupy 5-25% for a slope of 5-50% and soil bunds occupy 2-20% for a slope of 3-30% (Dabi *et al.*, 2017).

These practices involved both paid and unpaid labor, together representing an estimated investment of more than ETB 25 billion (or approximately USD 1.2 billion) per year over

the past 10 years. However, the outcomes in terms of impact on yield and livelihood benefits are yet to be fully understood (Adimassu et al., 2018).

Based on the overall consideration, the lack of integrated biophysical measures, absence of integration of indigenous practices, the lack of considering the socioeconomic profile, low perception and participation of farmers, the poor conservation design, improper land use, less maintenance, the weak monitoring and evaluation of soil and water conservation practices are the main constraints that determine the implementation of soil and water conservation in Ethiopia.

2.2 Sediment yield modeling

Based on the complexity and the level of dynamic physical processes that are implemented, models can be categorized into three different groups, namely empirical, conceptual, and physically-based models. Due to the increasing application of geospatial data, we further distinguish a fourth category: Remote Sensing and GIS-based modeling approaches (Raza et al., 2021). The complexity of modeling a non-linear process like rainfall-runoff conversion by any means is difficult and approximate. The more complex the model the more unwieldy the model fitting process will be (Pegram, & Sinclair, 2002).

The empirical models are more likely to be used with limited availability of input data. Contrary to that, physically-based models provide a physical description of the erosion process. These models are comparatively complex and less user-friendly because of their detailed depictions of processes and large data requirements. However, physically-based models are more capable when performing event-based simulations. Conceptual models typically have been developed for catchment and larger scales, requiring a general description of the catchment and involved soil erosion processes, without describing the details of their interactions that would require big data sets of temporal and spatially distributed catchment details. However, the United States, these equations are applied worldwide for soil loss estimations (Raza et al., 2021).

By contrast with more “physically based” models, the linear transfer function approach has the advantage that although we know it is an approximate model, it captures most of the important characteristics of the rainfall-runoff process - storage, losses, delays, topography, etc. The linear construct has the particular beauty of being relatively fast and simple to apply. The more complex the definition, the less precise the outcome. When it comes to a natural catchment where there are gross approximations used in the modeling, then the fitting of any model is fraught with difficulty, and the larger the number of parameters, the less precise their estimation (Pegram, & Sinclair, 2002).

Soil erosion processes strongly differ with spatial and temporal scales and environmental conditions. Thus, a large number of models have been developed that differ in terms of the processes considered, temporal and spatial application scale, capabilities, and limitations. It is worth indicating that some models were developed for soil erosion assessment at plot/field scale at daily time steps and some have the capability to account for rainfall interception but further improvements are required to deal with complex cropping systems. Most of the available soil erosion models have been developed mainly for larger scales (basin or watershed) where spatial variations in soil conditions (soil erodibility, soil cover, slope, and tillage practices) and hydrological conditions (surface runoff, infiltration rate, and rainfall intensity) are significant compared to those at small scales (field or plot) (Raza et al., 2021).

Among several methods, the sediment yield index (SYI) method and universal soil loss equation (USLE) are extensively used for the estimation of soil erosion and prioritization of watersheds for their treatment (Mishra et al., 2015). Most of the empirical models use the universal soil loss equation (USLE) and its derivates RUSLE and MUSLE. Though these equations have been developed using data obtained in the United States, these equations are applied worldwide for soil loss estimations (Raza et al., 2021). MUSLE has not yet been thoroughly validated in different regions for a good correlation between measured and MUSLE-predicted sediment yields. MUSLE may over-predict sediment yields for small events and under-predicted sediment yields for larger events. Modifying the coefficients of the runoff prediction model improved the accuracy of the model which tells that the problem may have been more with the hydrologic model used to synthesize runoff than with MUSLE perse (Jackson, et al, 1986).

The selection of a suitable model for a distinct purpose at the field scale should be guided by the following criteria. (1) Problem recognition: Define the problem statement in a clear

way to achieve a maximum match between the problem to be solved and the model objectives. (2) Spatial scale: the next criteria is to decide whether the model is compatible with the plot or field scale. (3) Data availability: make a list of required input data (topography, climate, field investigations) and their availability. (4) Temporal scales to be considered (event-based or continuous) (5) Elements to be assessed; decide which elements of the catchment are to be modeled i.e., overland erosion and sedimentation, hillslope erosion, or channel/stream erosion and sedimentation. (6) Model sensitivity; the uncertainties within input data should be identified that may impact the reliability of the simulated results before the model evaluation. (7) Model validation; simulation results must be compared with field observations that may also use for model calibration before the simulation process (Raza et al., 2021).

2.2.1 Modeling capabilities

Each soil erosion model has its predictive capabilities and modeling processes and its applicability depends on its intended use, available input and calibration data, temporal and spatial scale, and required accuracies (Raza et al., 2021).

The main advantages of MUSLE are its simplicity, the direct conceptual and physical relevance of its factors, the large database upon which the empirical relationship was developed, and the capability to insert management considerations into factor selection (Jackson, et al, 1986).

Most of the empirical models use the universal soil loss equation (USLE) and its derivates RUSLE and MUSLE. Models such as USLE, MUSLE, RUSLE, and MOSES have long-term simulation capabilities at both hillslope and catchment scales. MUSLE is capable of simulating erosion, prediction of sediment yield, and simulation of individual storm events (Raza et al., 2021).

2.2.2 Modeling limitations

Most of the models developed for large agriculture catchments using equations developed under specific conditions require site-specific calibration before simulation. Models designed for small-time steps perform better than continuous scale modeling. Similarly, calibration at a field or smaller scale, where spatial topographic and soil variations in the

erosion process greatly affect the simulation, is more accurate than that of larger catchment areas (Raza et al., 2021).

MUSLE also introduced three correction factors (slope length and gradient factor, crop cover factor, and water conservation measures factor) under different field conditions. It can be seen that soil loss quantity prediction accuracy depends on the above-mentioned parameters. However, not all parameters can be obtained by experimental measurement. Sometimes, we just indirectly estimate them by empirical model or statistical methods. Even the measured value often has an observational error due to limited conditions. These factors may lead to strong uncertainty in forecast results (An et al., 2016). Limited workability of these models was found for sediment transport, sediment deposit, and sediment yield (Raza et al., 2021).

The main disadvantages are that the model is empirical and does not consider all physical factors affecting sediment yield, and generally, there are fairly large errors associated with both soil loss (USLE) and runoff estimates (Jackson, et al, 1986). MUSLE is limited for calibrating simulation is complex, and shows a significant difference with measured sediment yield in many watersheds (Raza et al., 2021). An additional disadvantage in rangeland applications of MUSLE is that USLE erodibility factors are not as well developed for rangelands as for croplands (Jackson, et al, 1986).

According to Omar et al, (2018), the USLE, RUSLE, and MUSLE soil erosion models produced relatively similar results, however, the MUSLE model showed a higher spatial disputation of the erosion risk compared to the others. R factor was more effective in the MUSLE model; which explains the higher erosion rates obtained by this model. The comparison of the obtained results by the three models shows a very close value of the average rates. The coefficient of determination R2 between the results ranges from 93 to 98%, which confirms the strong correlation between the studied models.

2.2.3 Model improvement

The most important quality of the forecast is its accuracy. Expressed another way, the estimate of future flows may be made with great precision, but unless one knows how good the estimate is, it is relatively useless. There are two approaches to improving the forecasting ability. The first is to make more refined models with more intensive measurements to improve the estimates. The second is to improve the information collection instrumentation

for both rainfall and stream flows, and telemeter their measurements instantly to the flood control room. This up-to-the-minute information allows the model estimates to be continually adjusted to improve future forecasts. A combination of these two approaches will give the best results mindful of the need for relatively fast and straightforward computational procedures which the decision-makers can trust (Pegram and Sinclair, 2002).

Although the above-mentioned problems are significant, calibration of field scale models in fields characterized by spatial heterogeneity of topography and soil is more accurate than for larger catchment areas. Furthermore, the accuracy of the simulation of erosion rates depends on the spatial dimension taken into account, i.e., whether processes are simulated at the soil profile scale (1D, point-based assuming a field with homogeneous soil and terrain conditions) and/or spatially distributed method (2D/3D) (Raza et al., 2021).

Calibration aims to improve the predictive quality and fitness for use of erosion models for all these goals. However, we usually do not directly calibrate the processes we are attempting to predict. For instance, very often calibration is done on the discharge characteristics of a plot, catchment, or basin, assuming that if we manage to predict the hydrograph correctly, this is sufficient to predict accurately the sediment dynamics in the catchment. Whether this is feasible depends on several factors: availability and uncertainty of input data, the spatial complexity, the environmental setting, land use characteristics, and so on (Jetten and Maneta, 2011).

Calibrating the runoff model for the watershed, determining the relationship between peak flow rate and volume, and predicting sediment yield are activities required in the prediction of sediment yield. However, a measured runoff was used in these tests. Since measured runoff is rarely available in water resources planning, runoff is generally predicted with a hydrologic model. Thus, to properly evaluate the prediction accuracy of MUSLE predicted runoff is needed (Williams and Berndt, 1977). Sediment calibration must be done after the hydrologic calibration is completed, and it is extremely sensitive to the hydrology, particularly the amount and timing of surface runoff that is predicted by the model. Calibration of the parameters involved in the simulation of watershed sediment erosion is more uncertain than hydrologic calibration due to less experience with sediment simulation in different regions of the country (Donigian and Bicknell, 2006).

The MUSLE model has one unknown parameter that must be calibrated on a gaged watershed. Once calibrated, the model can be used to extend short periods (3 to 5 years) of record into long-term periods for the calibrated watershed or to predict water yield for nearby ungauged watersheds (Williams and Berndt, 1977).

The methods used at levels one and two involve two components: (1) evaluation of the "closeness" between the model outputs and the corresponding measurement data and (2) adjustment of the value of the parameter to improve the closeness. Manual (sometimes called expert) and automatic calibration techniques can be compared and contrasted in terms of how each of these components is implemented (Boyle et al., 2000).

Rarely is there, sufficient observed local data at sufficient spatial detail to accurately calibrate all parameters for all land uses and each stream and water body. Consequently, model users focus the calibration on sites with observed data and review simulations in all parts of the watershed to ensure that the model results are consistent with field observations, historical reports, and expected behavior from experience. This type of 'weight of evidence approach is rapidly becoming the standard practice in watershed modeling (Donigian and Bicknell, 2006).

The rationale for carrying out a validation study of the analytical calibration may be expressed as follows: to verify the reliability of the calibration scheme, via assessment of the accuracy and precision of the calibration and the analytical results yielded by it (Stauffer, 2018).

The quality and accuracy of the calibration of the erosion processes in heterogeneous fields should increase with the dimension that is considered. However, a major bottleneck for the multi-dimensional models is the availability and accuracy of soil information. On the other hand, the accuracy and availability of topographic information have considerably improved in the last decade (e.g., radar and laser-based sensors carried by UAV or airplanes) (Raza et al., 2021).

2.3 Sediment yield measurement on a hydrological gauging station

As indicated by WMO, (1994) the purpose of stream gauge stations is to provide systematic records of stage and discharge. Continuous streamflow records are necessary for the design

of water supply and waste systems, in designing hydraulic structures, in the operations of water management systems, and in estimating the sediment or chemical loads of streams, including pollutants.

However, except in limited circumstances, discharge cannot be measured both directly and continuously. Normal practice is to make periodic discharge measurements with concurrent measurements of the stage. A relationship is then obtained between stage and discharge which permits the conversion of a continuous stage record into a discharge record (DHV and DELFT, 2001).

A series of "instantaneous" discharge measurements can be made during flash flood conditions on small streams by rating individual subsections, or verticals. This method requires repeated observations of the height, depth, and velocity of the gauge in selected verticals during the rise and fall of the flood wave (Turnipseed and Sauer, 2010).

The stage of a stream or lake is the height of the water surface above an established datum plane. The water-surface elevation for most rivers and streams is measured above an arbitrary or predetermined gauge datum and is called the gauge height of the river or stream Stage or gauge height is usually in meters and hundredths or thousandths of a meter, or in feet and hundredths of afoot. The crest-stage gauge is a simple, economical, reliable, and easily installed device for obtaining the elevation of the flood crest (WMO, 2010).

Most discharge measurements are made by the current-meter method, also known as the area-velocity method because it is adaptable to a wide range of flow velocities and is practically unlimited to the total discharge which can be measured, provided the flow is not too turbulent (Tilrem, 1979), (Alberta, 2009).

The standard units for discharge measurement are m^3/s (cubic meters per second or cumecs). If we rewrite the units of discharge, we can think of them as a water velocity (m/s) passing through a cross-sectional area (m^2) (Davie and Quinn, 2019).

It is evident, that velocity observations must be made at a sufficient number of points to eliminate the effect of variations in the velocity of flow across the stream (Tilrem, 1979); (Alberta, 2009). For the velocity-distribution method, velocity measurements are made at several points in each vertical between the surface and the bed of the channel (DHV and DELFT, 2001).

The empirical, or also theoretical, relationship existing between the water-surface stage (i.e., the water level) and the simultaneous flow discharge in an open channel is known as the stage-discharge relation or rating curve, or also just rating. These expressions are synonymous and they can be used interchangeably. The rating curve is a very important tool in surface hydrology because the reliability of discharge data values is highly dependent on a satisfactory stage-discharge relationship at the gauging station (Braca, 2008).

Sediment load is the material being transported, and it can be divided into wash load and bed material load (Kitsikoudis *et al.*, 2013). The different phases of sediment transport generally occur simultaneously in natural streams, and there is no sharp line of demarcation between them. For convenience, sediment discharge is divided into two categories: suspended sediment and bed-material discharge. The latter consists of grains sliding, rolling, or saltating on or near the bed (WMO, 1994).

Annual and long-term sediment yields are generally much less valuable than within-storm sediment transport rates and daily or storm sediment discharges. However, the year-to-year variation in sediment yield variation for small watersheds can be great, if rainfall amounts,

intensities, and energies of the rainfall are variable, and if the seasonal occurrence of rainfall differs appreciably (Brakensiek *et al.*, 1979).

A dimensionless, commonly used measure for sediment quantification is concentration by weight in parts per million (ppm), which is the ratio of the sediment discharge to the discharge of the water-sediment mixture, both expressed in terms of mass per unit time (Kitsikoudis *et al*., 2013).

The basic principle of the methodology to predict sediment concentration is to estimate the annual sediment load at the point of interest and the amount of water that transports it. The amount of transported material is then redistributed in that corresponding water volume (using the flow characteristic) that determines sediment concentrations.

The sediment rating curve is a relationship between sediment concentration and discharge. Rating curves are used to calculate or predict a variable that is difficult to measure continuously (Najib *et al.*, 2020).

The graphical relation of water discharge versus sediment discharge or concentration from a watershed is called the sediment transport rating curve or sediment rating curve. It can be prepared in many forms and is often used for estimating missing periods of record and for the extrapolation of sediment yields (Brakensiek *et al.*, 1979).

Transport-curve relations are usually defined as a power function. As Balamurugat, (1989) adopted from Sieh & Sivapakianathan, (1977) and Peh (1981), the most common form of relationship assumed to exist between river discharge and sediment concentration or load for Malaysia as

$$c = aQ^b \text{ or } \quad L = aQ^b \qquad Eq\ 2\text{-}1$$

where C = suspended sediment concentration in mg/l, L = suspended sediment load in tones/day Q = river discharge in cumecs, a = coefficient, b = exponent (Gray *et al.*, 2008), (Balamurugat, 1989).

2.4 Data acquisition tools for sediment yield modeling

The use of geographical data is progressively becoming important for all government and non-government sectors for different special and general uses. From those sectors, Agricultural Development offices are currently using ArcGIS and Google earth software for different purposes like land use classification, slope map, soil map, and development map preparation (Mohammed, 2017), earth resource mapping, visualizing earth features, 3-D renderings of structures, town planning, simulation of disaster events such as earthquakes using the Google Earth model, monitoring traffic speeds and congestion, etc. (El-Ashmawy, 2016).

Geographic information systems (GIS) can be used to estimate watershed features, such as watershed boundaries and drainage areas; flow path lengths and slopes; stream and flood plain reach lengths; average watershed land slopes; land cover; and, in some cases, stream cross-sectional features. This information can then be imported into several hydrology computer programs, which use the data to estimate times of concentration for watersheds (IDNR, 2009).

Using Google Earth imagery by digitizing after geo referencing for land use classification was one step higher than using old low-resolution Landsat images. But geo-referencing was the main obstacle to working easily which requires more time to take readings from the field and put it on the specified points to make images geographically referenced. But classifying

all land uses on Google earth pro and importing it into ArcMap with its compatibility to do all ArcMap features are more simplified and easier to work (Mohammed, 2017).

GE has a different discriminating capacity for specific land use/cover types. It possesses some advantages for mapping those types with good spatial characteristics in terms of geometrics, shape, and context. The object-based method is recommended for imagery classification when using GE imagery for mapping land use/cover. However, GE has some limitations for those types classified by using only spectral characteristics largely due to its poor spectral characteristics (Hu *et al.*, 2013).

The spatial resolution of the raw DEM matters how our hydrologic analysis is accurate and represents the real hydrologic properties of the catchment. But the availability of better resolution DEM and even access to the free online DEM data may be difficult for some experts and planners (Mohammed, 2017).

Google Earth uses digital elevation model (DEM) data collected by NASA's Shuttle Radar Topography Mission (SRTM) enabling a 3D view of the whole earth. Google Earth also supports managing 3D Geospatial data through Keyhole Markup Language (KML) (El-Ashmawy, 2016).

The available digital elevation models on a regional level have a resolution of a minimum of 20 meters and this may not enough for analyzing our small catchment's hydrology. Using google earth pro, a GPS visualizer website, and ArcGIS or QGIS software the problem of resolution can be minimized and we can create out digital elevation model (Mohammed, 2017) With a stronger correlation the DEM derived from Google Earth is relatively as acceptable as DEMs from ASTER and SRTM data sources (Rusli *et al.*, 2014). The Google

Earth pro was also concluded to perform far better than the SRTM 30 data (Isioye *et al.*, 2012).

GPS receivers provide a fast and convenient method for obtaining position information that can be collected in real-time and is easily employed within a GIS (Taylor *et al.*, 2000). It is being used all over the world for numerous navigational and positioning applications, including navigation on land, in the air & at sea, determining the precise coordinates of important geographical features as an essential input to mapping and Geographical Information systems (GIS), along with its use for precise cadastral surveys, vehicle guidance in cities and on highways using GPS-GIS integrated systems, earthquake and landslide monitoring, etc. (Kulkarni, 2003). It can be used to record the times and locations of each activity and the trips in between (McGowen and McNally, 2007). They can be used for navigation, mapping, or surveying (CNWD, no date).

GIS can perform an Overlay, Neighborhood, Connectivity, Classification retrieval, and measurement analytical functions (By De *et al.*, 2001). A key benefit of geographic information systems (GIS) is the ability to apply spatial operators to GIS data to derive new information; These tools form the foundation for all spatial modeling and geoprocessing; Of the three main types of GIS data—raster, vector, and tin—the raster data structure provides the richest modeling environment and operators for spatial analysis (ESRI, 2002).

It can provide answers to simple spatial questions such as How steep is it at this location? and What direction is this location facing? It can also find answers to more complex spatial questions such as Where is the best location for a new facility? and What is the least costly path from A to B? The comprehensive set of Spatial Analyst tools within ArcGIS allows you to explore and analyze your spatial data and enables you to find solutions to your spatial

problems. It is possible to run tools from the Spatial Analyst toolbox or the Python Window, accessible via any ArcGIS Desktop application (ESRI, 2010).

The three interpolation algorithms widely used in geo-statistics are the Thiessen Polygon Method, Universal Kriging (UK), and Inverse Distance Weighting (IDW) (Mei *et al*., 2012), (Garnero and Godone, 2013). All combine information about the sample coordinates with the magnitude of the measurement variable to estimate the variable of interest at the unmeasured location (Wu, 2019).

Thiessen Polygon Method assigns interpolated value equal to the value found at the nearest sample location. Often called the nearest sample or nearest neighbor. Accuracy depends largely on sampling density (Wu, 2019).

Inverse Distance Weighted IDW estimates cell values by averaging the values of sample data points in the vicinity of each cell. The closer a point is to the center of the cell is estimated the more influence, or weight it has in the averaging process (ESRI, 2002). IDW Estimates the values at unknown points using the distance and values to nearby know points (IDW reduces the contribution of a known point to the interpolated value). The weight of each sample point is an inverse proportion to the distance (Wu, 2019).

IDW directly implements the assumption that a value of an attribute at an unsampled location is a weighted average of known data points within a local neighborhood surrounding the unsampled one (Garnero and Godone, 2013). With Inverse Distance to a Power, data are weighted during interpolation, so that the influence of one point, relative to another, declines with distance from the grid node. Weighting is assigned to data through the use of a weighting power, which controls how the weighting factors drop off as the distance from the grid node increases. The greater the weighting power, the less effect the points, far removed

from the grid node, have during interpolation. As the power increases, the grid node value approaches the value of the nearest point (Yang *et al.*, 2004).

Garnero and Godone, (2013) indicated that The Inverse Distance Weighing (IDW) interpolator is an automatic and relatively easy technique, as it requires very few parameters from the operator, such as search neighborhood parameters, exponent, and eventually smoothing factor, from the operator. The process is highly flexible and allows estimating datasets with trend or anisotropy, in search of neighborhood shaping.

Kriging is a geostatistical gridding method that has proven useful and popular in many fields (Yang *et al.*, 2004). Kriging was originally developed in geostatistics by South African mining engineer D.G.Krige (Mei *et al.*, 2012). This method produces visually appealing maps from irregularly spaced data. Similar to Inverse Distance Weighting (IDW) Kriging uses the minimum variance method to calculate the weights rather than applying an arbitrary or less precise weighting scheme. A statistical-based estimator of spatial variables (Wu, 2019).

Kriging attempts to express trends suggested in your data, so that, for example, high points might be connected along a ridge rather than isolated by bull's-eye type contours. For a set of regionalized variables Z(x), Kriging estimates the expected value Z (x 0) at location x 0 where the observation is not available using a linear weighted sum of the known values Z (x 1), Z (x 2), ..., Z (x n) at locations x 1, x 2, ..., x n, such that: (Mei, Tipper and Xu, 2012). Kriging is a very flexible gridding method. The Kriging defaults can be accepted to produce an accurate grid of your data, or Kriging can be custom-fit to a data set, by specifying the appropriate variogram model. Within SURFER, Kriging can be either an exact or a smoothing interpolator, depending on the user-specified parameters. It incorporates anisotropy and underlying trends efficiently and naturally (Yang *et al.*, 2004).

A key issue in the UK is to calculate variograms; the rate at which the variance between points changes over space (Mei *et al.*, 2012), (Haithcoat, 1999) in which experimental variograms are estimates of the theoretical ones. The variograms are calculated for a set of vectors that is the distance of any pair of observations (Mei *et al.*, 2012).

In developing the variogram it is necessary to make some assumptions about the nature of the observed variation on the surface. Simple Kriging assumes that the surface has a constant mean, no underlying trend and that all variation is statistical and Universal Kriging assumes that there is a deterministic trend in the surface that underlies the statistical variation. In either case, once trends have been accounted for (or assumed not to exist), all other variation is assumed to be a function of distance. The input data for Kriging is usually an irregularly spaced sample of points and to compute a variogram we need to determine how variance increases with distance (Haithcoat, 1999).

It is a geostatistical method that basis on a statistical model that enables it to produce a prediction surface with some measure of certainty and accuracy (ESRI, 2002).

The difference between IDW and Kriging is that they calculate the weights variously (Mei *et al.*, 2012). There is no absolute best method but only the optimal choice under certain circumstances. One should first review the characteristics and theorem of each method as well as the property and spatial analysis of data before he or she can successfully select a spatial interpolation method that is relatively best in certain situations (Yang *et al.*, 2004).

3 MATERIALS AND METHODS

3.1 Description of the study area

3.1.1 Location and topography

The study area Agewmariam watershed was established as an experimental watershed in 2016 to research soil and water conservation on a watershed scale pretending it can represent well the surrounding ecological, biophysical, and socioeconomic conditions. It is located in Sayda kebele; 23 km southwest of Sekota town in Waghimra administrative zone of Amhara regional state in Ethiopia. It is a part of the Tekeze river basin; covering 155.39 ha; located between 12º 31’ 40” -12º 32’33” N Latitudinal and 38º 55’ 14”-38º 56’ 15” E Longitudinal range. The Watershed elevation ranges from 2109 to 2381 m above sea level and the land slope ranges from nearly flat (<3%) to extremely steep slope (>50%).

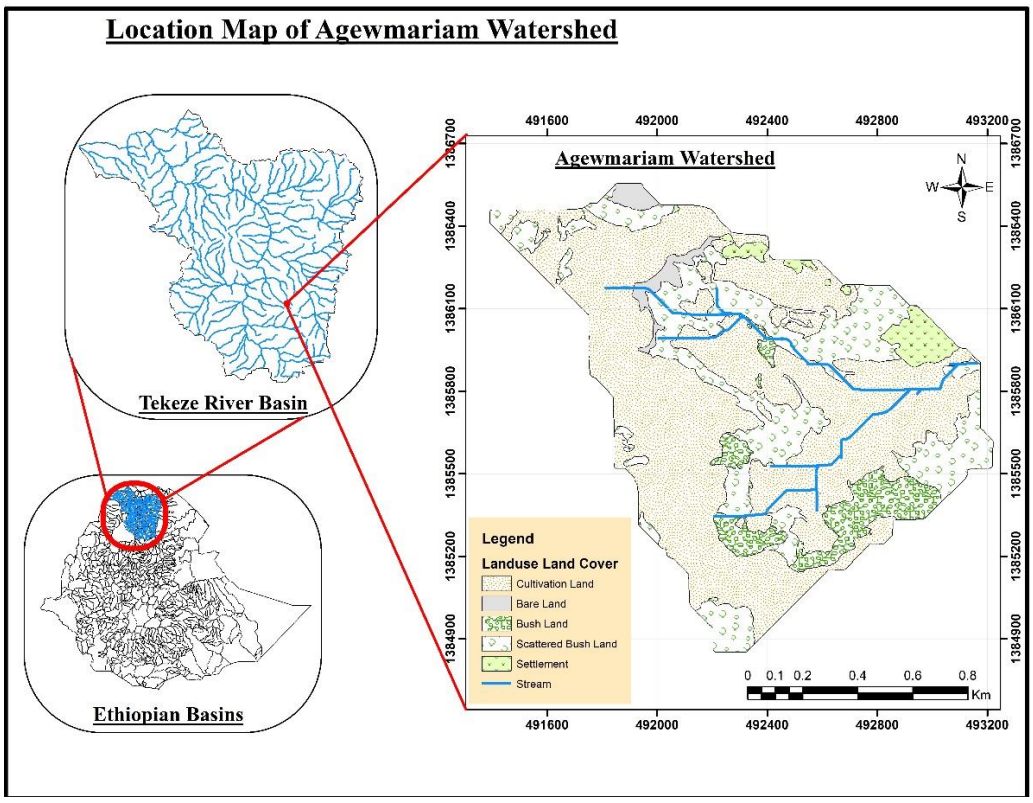

Figure 3-1 Location Map of Agewmariam Watershed

3.1.2 Climate

The study area is characterized by a Dry-Woina-Dega agroecological zone based on the classification of Hurni et al., (2016); with an altitudinal range from 2109 to 2381 m above sea level. It has a unimodal rainfall pattern, in which the main rainfall season extends from late June to early September while the dry season extends from October to May. The rainfall is known for its erratic distribution. The mean annual rainfall of the area is 679 mm and the mean minimum and maximum annual temperatures are 12.5 °C and 26.5 °C, respectively (NMA, 2019).

3.1.3 Socio-economic characteristics

The watershed is inhabited by a total of 1113 individuals and 259 households inside and around the watershed. The average family size in the community was 4 people per household. It is characterized by five major land-use types such as cultivation land, bare land, dense bush, scattered bush, and settlement with area percent coverage of 63.3%, 2.0%, 7.2%, 24.7%, and 2.8% respectively.

The major and active source of income was crop production, livestock raring, labor, and food aid. They produce food crops and follow a free grazing animal rearing which was the dominant source of economic income. The most dominantly grown crops are sorghum, barley teff, and wheat. The average arable land holding size is 0.5 ha.

The main source of feed for animals is the crop residue and some hey collected from farm boundaries. Overexploitation and inappropriate uses of land resources in the study watershed resulted in the process of severe soil erosion, which is the major challenge to keeping stable and productive ecosystems in the study area.

3.2 Data Collection

Agewmariam watershed is a newly established watershed with no database. Modeling and evaluation of the MUSLE model required the collection analysis and establishment of both measured (observed) and estimated input databases. So, important data were collected from field surveys, measurements, and Google Earth, and some are adopted from literature or generated by GIS or other analyses.

A transect walk was held on across the watershed and good observations have been made to have a general mental map of land use and land feature of the watershed. Biophysical data from the watershed, such as slope, soil depth, Stoniness, past erosion severity, land use type, and texture, including soil samples were collected from 155 points of sampling with a 100m*100m fixed grid using a GPS navigation tool. Soil samples were collected using an auger for the top 30 cm soil depth physical and chemical property determination.

Google Earth Pro was used for land use land cover classification and high-resolution DEM (2m*2m) preparation. Image from Google earth pro © 2019 CNES/ Airbus was digitized to map the land use land cover.

Daily Precipitation data was collected from a manual rain gauge installed inside the watershed.

Figure 3-2 Manual rain gauge in the watershed

For sediment loss measurement; runoff depth and velocity were measured using a broad crested rectangular weir and flow meter installed at the outlet of the watershed. Runoff samples were collected for the determination of suspended sediment load.

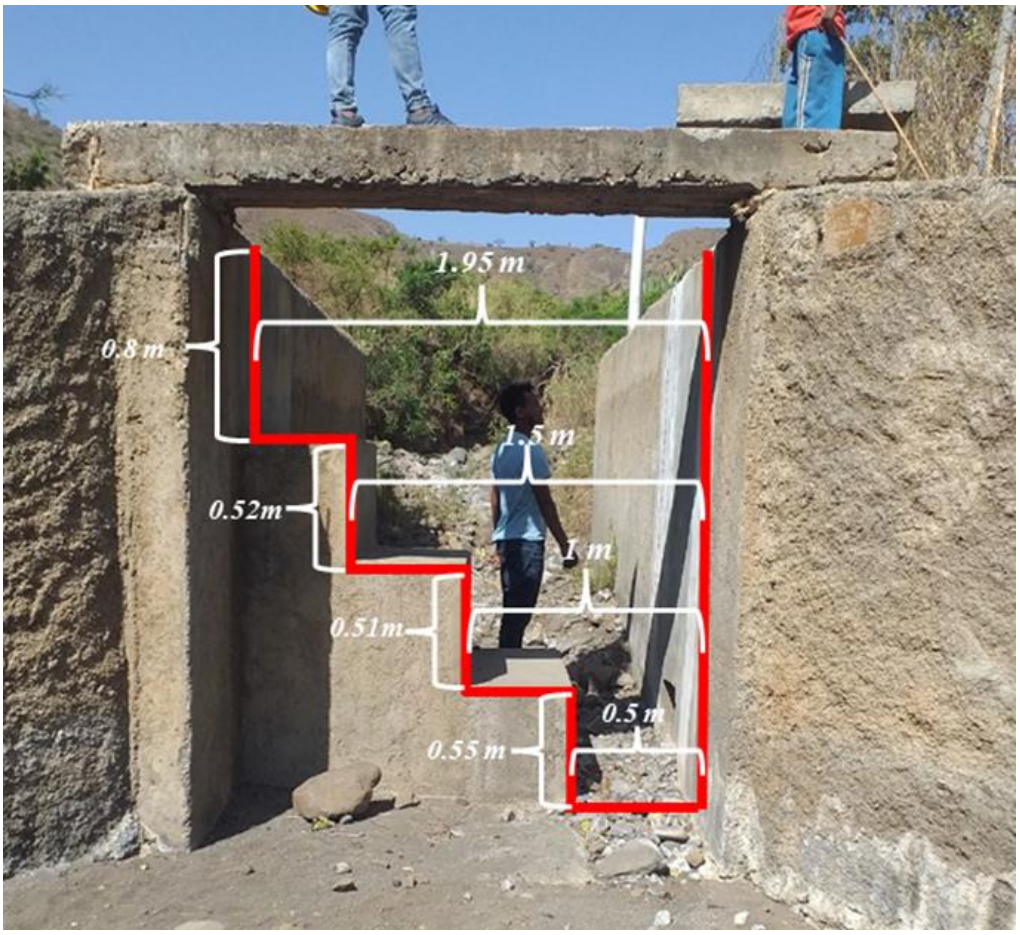

Figure 3-3 Hydrologic monitoring weir (Agewmariam WS)

3.3 Data analysis

3.3.1 Sediment Yield Measurement and Analysis

First runoff depth was recorded manually using a graduated mark on the sidewall of the weir. Runoff depth is the Gauge height; which is often used interchangeably with the more general term stage, although the term gauge height is more appropriate when used with a specific reading on a gauge. The cross-section area of the channel at the measurement point for each respective runoff depth was determined using (Eq 3-1).

$$A = \sum_{i=1}^{n} Di * Wi \qquad \text{Eq 3-1}$$

Where A_t = Total cross-section area, D_i = Depth of the i^{th} cross-section and W_i = Width of the i^{th} cross section (Alberta, 2009).

Second runoff flow velocity at a repeated number of points in the vertical was measured and recorded using a high-quality; factory-calibrated Global Water Flow Probe. It is evident, that velocity observations must be made at a sufficient number of points to eliminate the effect of variations in the velocity of flow across the stream (Tilrem, 1979); (Alberta, 2009). The average velocity for each respective depth was determined.

Third, the velocity–area method was used for discharge measurement (Davie and Quinn, 2019). Tilrem, (1979), and Davie and Quinn, (2019) defined Stream discharge as the product of velocity and cross-sectional area of flow and this method evaluates these two terms for a particular cross-section at a particular time. The flow rate and runoff volume were calculated using (Eq 3-2) and (Eq 3-3) (Alberta, 2009).

$$Q = \sum_{i=1}^{n} Vi * Ai \qquad \textit{Eq 3-2}$$

Where Q is the flow or discharge (m^3/s), v is the velocity measured in each cross-sectional area, and A is the cross-section area of the channel on each step of the weir (Alberta, 2009), (Davie and Quinn, 2019). The stream discharge is the sum of the discharges in all the sub-sections.

$$Qv = Q * t \qquad \textit{Eq 3-3}$$

Qv = Volume of runoff, Q = Discharge and T = Duration of flow (Alberta, 2009).

For the suspended sediment concentration determination in the laboratory analysis, the sediment was separate from the runoff samples using filter paper and weighed on a sensitive balance.

Figure 3-4 sediment filtering and weighing in a laboratory.

Sediment yield, together with the amount of water available to transport the material, also primarily determines sediment concentrations (Bečvář, 2006).

$$\boldsymbol{Sediment\ Conxentration}\ (\boldsymbol{g/l}) = \frac{\boldsymbol{Transported\ Material}\ (\boldsymbol{g})}{\boldsymbol{Water\ Volum}\ (\boldsymbol{l})} \qquad \boldsymbol{Eq\ 3\text{-}4}$$

The concentration of suspended sediment samples can be determined by either evaporation or filtration. The filtration method consists of filtering the sample through an appropriate filter and oven-drying the filter together with the filtered sediment (Tilrem, 1979).

Suspended sediment concentrations should be reported in terms of the dry weight of sediment per liter of a sample (water-sediment mixture), in milligram per liter (mg/1). For convenience in the laboratory, the concentration is calculated by dividing the weight of dry sediment by the weight of the sample and expressing the result in parts per million (ppm). If, for example, the sample weighs 400 grams and the amount of dried sediment is 0.02 grams, the concentration of sediment would be 0.02 grams in 400 grams which is the same

as 50 grams in 1,000,000 grams or 50 ppm. Parts per million are calculated as one million times the ratio of the dry weight of sediment in grams to the weight of the sample in grams. Then, the conversion from ppm to mg/1 is done to the ppm values as follows:

$$^{mg}/_{l} = C * (ppm) \qquad \textit{Eq 3-5}$$

It is recommended that sediment concentration is reported to the nearest 0.1 mg/l up to 9.9 mg/1, for values ranging from 10 mg/1 up to 999 mg/1 the concentration should be reported to the nearest 1 mg/1, for higher values three significant figures should be used. These recommendations are based on the assumption that the net sediment can be weighed to the nearest 0.1 mg and the water-sediment mixture to the nearest 1 gram (Tilrem, 1979).

3.3.2 MUSLE model parameter determination and analysis

Except for substituting the runoff energy factor for the rainfall energy factor in USLE the remainder of the equation is identical to USLE (Smith *et al.*, 1984). USLE requires delivery ratios because the rainfall factor represents the energy used in detachment only. Delivery ratios are not needed with MUSLE because the runoff factor represents the energy used in detaching and transporting sediment (Williams and Berndt, 1977), (Gwapedza *et al.*, 2021).

The MUSLE is expressed as

$$Y = 11.8(Q * qp)^{0.56} KLSCP \qquad \textit{Eq 3-6}$$

Where: Y = the sediment yield from an individual storm in metric tons, Q = the storm runoff volume in m^3, qp = the peak runoff rate in m^3/sec, K = the soil-erodibility factor, LS = the slope length and gradient factor, C = the crop management factor, and P = the erosion-control-practice factor.

Runoff Energy Factor Analysis

Determination of the runoff energy factor was the first attribute to be worked on. This factor by itself was attributed to two subfactors; which are runoff depth and peak discharge. For the estimation of runoff discharge and runoff peak discharge, the NRCS curve number method and the SCS graphical peak discharge estimation methods were respectively used.

The energy factor in MUSLE is represented by the equation as

$$\boldsymbol{E = 11.8(Q * qp)^{0.56}} \qquad \text{Eq 3-7}$$

Where Q is the predicted runoff depth in mm and qp is the predicted runoff discharge m^3/s.

Runoff Depth (Q_d)

The following procedures were used to compute the runoff depth and peak discharge. To compute the runoff depth, first, the watershed boundary and area coverage were determined on the ArcGIS environment using the Arc SWAT extension. Second, the slope distribution of the watershed area was mapped on Arc GIS from a DEM of 2m*2m resolution. Third, the land-use type for all the HRUs was mapped Using ArcGIS and Google Earth Pro. Fourth, the amount and type of rainfall are defined from a measured rain gauge value and different literature. Fifth, the runoff curve number (CN) for each HRU was determined by considering the land use type, slope class, agricultural practice system, and antecedent soil moisture content. To determine the curve number (CN), the HRUs in the watershed are identified by overlaying the slope map, land use map, and soil hydrologic group. Based on the HRU the curve number value was read from (**Error! Reference source not found.**) and (Appendix table 2) and then the CN values for the antecedent moisture condition I and III were calculated using equations (Eq 3-8) and (Eq 3-9) Respectively.

The formulas used by (Mishra and Singh, 2003) to determine the curve number value for each antecedent moisture condition are given as follows.

$$CN_{ARC(I)} = \frac{CN_{ARC(II)}}{\left(2.281 + 0.01281 * CN_{ARC(II)}\right)} \qquad \textbf{Eq 3-8}$$

$$CN_{ARC(III)} = \frac{CN_{ARC(II)}}{\left(0.427 + 0.00573 * CN_{ARC(II)}\right)} \qquad \textbf{Eq 3-9}$$

Where CN is the curve number, ARC(III) is the antecedent runoff condition three, ARC(II) is the antecedent runoff condition two, and ARC(I) is the antecedent runoff condition One (Mishra and Singh, 2003),(Chow *et al.,* 1988).

Then the runoff depth was calculated as

$$Q = (\boldsymbol{P - 0.2S})^2/(\boldsymbol{P + 08S})\ \ \boldsymbol{p \geq \lambda S} \qquad \textbf{Eq 3-10}$$

(Eq 3-10) has an advantage over many others that have been proposed. It is easier to use because it requires only one parameter (S) related to the characteristics of the watershed. S is related to the curve number by the relationship

$$S = \frac{1000}{CN} - 10\ for\ British\ Unit\ OR\ S = \left(\frac{1000}{CN} - 10\right) * 25.4\ for\ SI\ Unit\ System \qquad \textbf{Eq 3-11}$$

Where S is in inches or mm (NRCS, 2004).

Peak Discharge (Qp)

To compute the runoff peak discharge the following procedures were used. First, the time of concentration (tc) for the longest path in the watershed was calculated using the NRCS/SCS velocity method.

For the sheet flow segment, the simplified version of Manning's kinematic solution equation (Eq 3-12) was used.

$$T_t = \frac{0.007(nl)^{0.8}}{(P_2)^{0.5} S^{0.4}} \qquad \textbf{Eq 3-12}$$

Where: T_t = Travel Time (h), N = Manning's roughness coefficient (Appendix table 5), *l* = Sheet flow length (m), P_2 = 2-year, 24-hour rainfall (mm), S = slope of land surface (m/m)

Manning's roughness coefficient for sheet flow was estimated using (Appendix table 5).

For the shallow concentrated flow, the average velocity was determined using a graph (Appendix figure 1) based on the slope and land use type and turned into travel time using (Eq 3-13*).*

$$T_t = \frac{l}{3600 * V} \qquad \textbf{Eq 3-13}$$

Where: T_t = Travel time (h), L =Distance between the two points (m), V = Average velocity of flow between the two points (m/s), 3600 = A conversion factor to change seconds to hours.

The open channel flow was calculated using manning's equation (Eq 3-14*).*

$$V = \frac{1.49 r^{\frac{2}{3}} S^{\frac{1}{2}}}{n} \qquad \textbf{Eq 3-14}$$

$$r = \frac{a}{P_w} \qquad \textbf{Eq 3-15}$$

V = Average Velocity, (ft/s), R = Hydraulic radius, (ft), A = Cross-sectional flow area, (ft^2), Pw = wetted perimeter, (ft), S = slope of hydraulic grade line (channel slope), (ft./ft.), M =

Manning's roughness coefficient for open channel flow was estimated using (Appendix table 6).

Then the travel time for each segment was summed up to give the time of concentration (Tc); as shown in equation (Eq 3-16).

$$T_c = T_{t1} + T_{t2} + \cdots T_{tn} \qquad \textbf{Eq 3-16}$$

Where: Tc = Time of Concentration (h), T_{tn} = Travel time of segment n (h), N = number of segments comprising the total hydraulic length.

Second, the unit peak discharge (qu) was computed using equation (Eq 3-17) based on the time of concentration, type of rainfall distribution, and given regression coefficients.

The determination of the peak discharge in the graphical peak discharge estimation method needs the determination of the basic component so-called unit peak discharge which can be determined using the following equation (Cronshey *et al.*, 1986).

$$q_u = 10^{[C_0+(C_1)(\log t_c)+(C_2)(\log t_c)^2]} \qquad \textbf{Eq 3-17}$$

Where C0, C1, C2 = Coefficients, tc = time of concentration

A conversion factor of 0.0000043 will be used to convert ft^3 / s /mi^2 / in in to m^3 / s / ha /mm (Tollner, 2016)

Third, the peak discharge (q p) was calculated using equation (Eq 3-18) based on the time of concentration and regression coefficient considering a type II rainfall distribution.

$$q_p = q_u * A_m * Q_d * F_P \qquad \textbf{Eq 3-18}$$

Where; qp= Peak flow, qu = Unit peak flow, Am = Basin area, Qd = Runoff depth, and Fp = Pond and swamp adjustment factor (Cronshey *et al.*, 1986).

At the time of the field survey observations of soil condition, land use type, slope, stoniness, and the channel system were made and noted. This information was used in the estimation of curve number and roughness coefficient.

Soil erodibility (K) factor

The soil erodibility factor K represents the susceptibility of soil to erosion, transportability of the sediment, and the amount and rate of runoff given a particular rainfall input, as measured under the standard unit plot condition (Renard *et al.*, 1997). It is the soil loss rate per erosion index unit for a specified soil as measured on a standard condition or unit plot, which is defined as a 72.6-ft (22.13 m) length of uniform 9-percent slope maintained in continuous fallow, tilled up, and downhill periodically to control weeds and break crusts that form on the surface of the soil (Renard *et al.*, 1997), (Wischmeier and Smith, 1978).

The collected soil samples were sent to the soil laboratory for the determination of the texture and soil chemical properties of pH, EC, OM, and OC. soil samples were analyzed using standard laboratory procedures. Particle size distribution (texture) was determined using the hydrometer method, whereas organic carbon was determined by the wet combustion method

The soil erodibility factor, K, was calculated for the topsoil layer using equation (Eq 3-19) based on field measurement of soil sand silt and clay fraction and soil organic carbon.

In the absence of soil structure and soil hydraulic conductivity data the equation (Eq 3-19) can be used to calculate K. The soil erodibility factor, K is evaluated for the topsoil layer at the start of each year of simulation with the equation.

$$K = \left(0.2 + 0.3exp\left(-0.0256\,SAN\left(1 - \frac{SIL}{100}\right)\right)\right)\left(\frac{SIL}{CLA + SIL}\right)^{0.3} \ldots\ldots\left(1.0 - \frac{0.25\,C}{C + exp(3.72 - 2.95\,C)}\right) \ldots\ldots\left(1.0 - \frac{0.7\,SN1}{SN1 + exp(-5.51 + 22.9\,SN1)}\right) \quad \textbf{Eq 3-19}$$

Where SAN, SIL, CLA, and C are the sand, silt, clay, and organic carbon of the soil and SN1=1-SAN/100. (Eq 3-19) allows K to vary from about 0.1 to 0.5. The first term gives

low K values for soils with high coarse-sand contents and high values for soils with little sand. The fine sand content is estimated as the product of sand and silt divided by 100. The expression for coarse sand in the first term is simply the difference between sand and the estimated fine sand. The second term reduces K for soils that have high clay to silt ratios. The third term reduces K for soils with high organic carbon content. The fourth term further reduces K for soils with extremely high sand contents (SAN>70 %) (Sharpley and Williams, 1990).

The point data collected from the field were interpolated to give a raster map using ordinary kriging interpolation.

Slope length & steepness (LS) factor

The slope-length factor is the ratio of soil loss from the field slope length to that from a 72.6-ft length under identical conditions. The slope-steepness factor is the ratio of soil loss from the field slope gradient to that from a 9 percent slope under otherwise identical conditions (Wischmeier and Smith, 1978).

The S-factor measures the effect of slope steepness, and the L-factor defines the impact of slope length. The combined LS factor describes the effect of topography on soil erosion (Panagos *et al.*, 2015).

The slope length factor L computes the effect of slope length on erosion and the slope steepness factor S computes the effect of slope steepness on erosion. Values for both L and S equal 1 for the unit plot conditions of 72.6 ft length and 9 percent steepness. Values of L and S are relative and represent how erodible the particular slope length & steepness are relative to the 72.6 ft long, 9 percent steep unit plot. Thus, some values of L and S are less than 1, and some values are greater than 1.

The standard definition of slope length is the distance from the origin of the overland flow along its flow path to the location of concentrated flow or deposition (Renard *et al.*, 1997).

The slope-length factor was calculated using equation (Eq 3-21) from a DEM of 2m*2m resolution.

The LS factor is computed with the equation

$$LS = \left(\frac{L}{22.1m}\right)^{m} (0.065 + 0.045S + 0.0065S^{2}) \qquad \textbf{Eq 3-20}$$

For a GIS application, the formula is rewritten as

$$LS = \left(\frac{Flow\ accumulation * Cell\ resolution}{22.1m}\right)^{m} (0.065 + 0.045S + 0.0065S^{2}) \qquad \textbf{Eq 3-21}$$

m = 0.5 if the percentage of the slope is 5 or more, 0.4 on slopes of 3.5 to 4.5 percent, 0.3 on slopes of 1 to 3 percent, and 0.2 on uniform gradients of less than 1 percent (Wischmeier and Smith, 1978), (Girmay *et al.*, 2020), (Alemayehu *et al.*, 2019).

As a procedure to generate a high-resolution DEM; activities of Creating a fishnet point shapefile of the watershed with a 2 m*2m meter space grid on Arc GIS environment, importing shapefiles to Google Earth, collecting elevation points data from Google earth to convert by adding elevation KML data into www. gpsvisualizer.com and Converting the point data into digital elevation model were conducted (Mohammed, 2017).

Using the DEM, a slope map was generated using ArcGIS 10.7, and (Eq 3-21) was used to calculate the slope length and steepness factor value.

Cover management (C) factor

The cover & management factor is the ratio of soil loss from an area with specified cover and management to that from an identical area in tilled continuous fallow (Wischmeier and Smith, 1978).

The C factor values were adopted from reported values for similar land use types as listed in (Appendix table 8). To create a land use land cover map, a watershed boundary shapefile was created on ArcGIS and imported into Google Earth Pro, adding features and land cover classifications on Google Earth, exporting digitized features from Google Earth to the GIS environment, after conversion and projection; extracting necessary information was done. Further tasks like area calculation, overlay of the slope, soil, and other relevant layers were done (Mohammed, 2017).

Support practice factor (P)

The support practice factor is the ratio of soil loss with a support practice like contouring, strip cropping, or terracing to that with straight-row farming up and down the slope (Wischmeier and Smith, 1978).

Like the C factor values, the P factor values were taken from a literature table; (Appendix table 9) based on the slope and terrace practice.

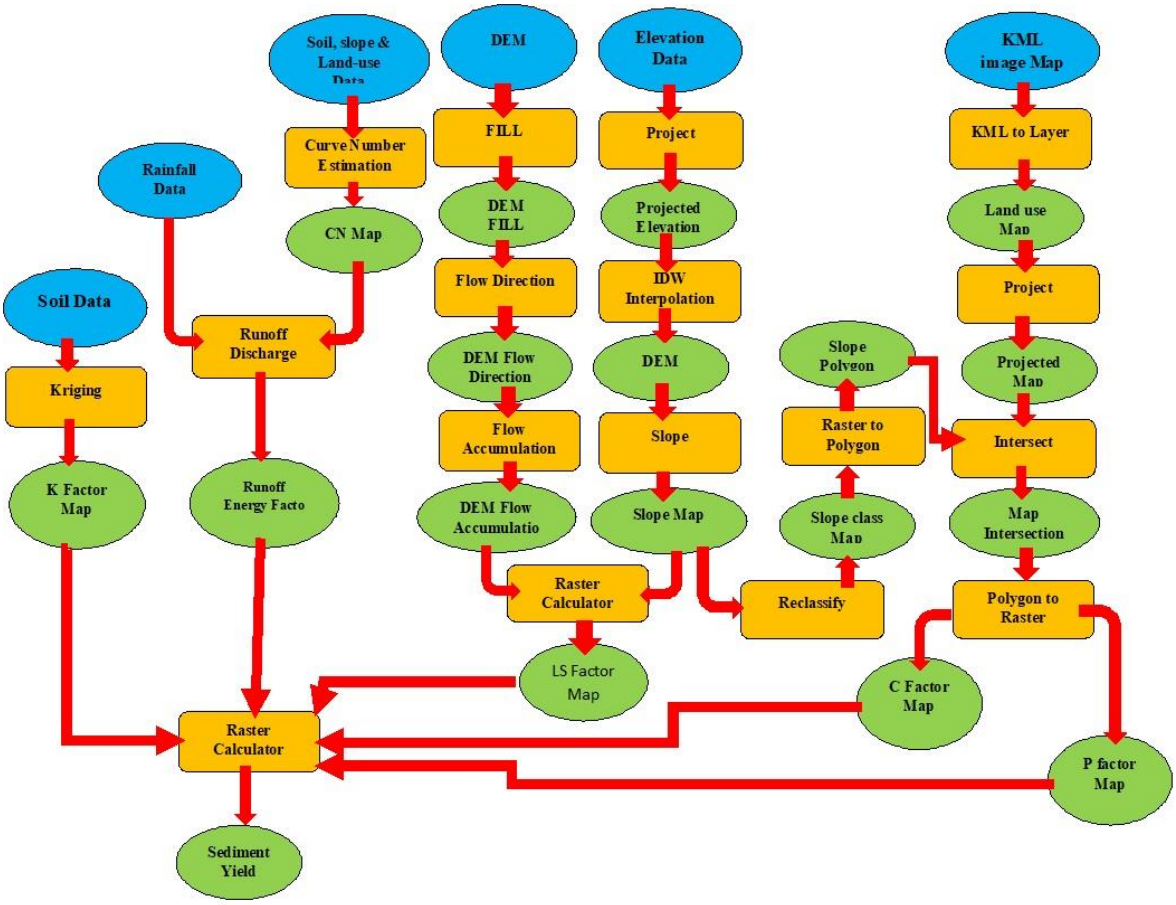

Figure 3-1 Flow chart of the modeling process

3.3.3 Model calibration, validation, and evaluation

Calibration

Calibration is the process of bringing a task, method, procedure, or some operation, in general, into conformity with a set of objectives and goals that are solidly established and highly reliable; that is, based on information that is precise and accurate (Stauffer, 2018).

An iterative approach was used for manual calibration of the curve number values to obtain the best fit of rainfall-runoff generation; peak discharge and sediment load using the formulas and equations in the MS-excel worksheet between the measured and simulated values involving the following steps.

First, Model simulation was performed; Second, Measured and simulated values were compared to assess the reasonability of the results; Third, The input parameters were then adjusted based on expert judgment and guidance of result values within reasonable parameter value ranges by repeating the process until it is determined that the best fitting results have been obtained (Arnold *et al.*, 2012).

As noted above, sediment yield model calibration for the watershed involved numerous steps, from initial estimates of model parameters, all the way to mimicking transport behavior within the channel system and at the watershed outlet.

These steps included are; Estimating target (or expected) sediment loading rates from the landscape, often as a function of topography, land use, and management practices, Calibrating the model loading rates to the target rates, scour, deposition, and transport parameters were adjusted for the stream channel to mimic the expected behavior of the streams/water bodies, sediment bed behavior analyzed and transport in each channel reach compared to field observations, overall sediment budgets for the land and stream contributions were analyzed, along with stream aggrading and degrading behavior throughout the stream network, simulated and observed sediment concentrations were compared, including particle size distribution information, and load information where available and steps 1 through 6 were repeated as needed to develop a reasonable overall representation of sediment sources, delivery, and transport throughout the watershed system (Donigian and Bicknell, 2006).

Validation

Model validation is the process of demonstrating that a given site-specific model is capable of making sufficiently accurate simulations, although ‘sufficiently accurate’ can vary based

on project goals. Validation involves running a model using parameters that were determined during the calibration process and comparing the predictions to observed data not used in the calibration (Moriasi *et al.*, 2007). For the validation, a model simulation was run using data different from the data used for the calibration period.

Sensitivity analysis

A sensitivity analysis is a process of assessing which model input parameters have the greatest effect on the predictions made with the model. Water budgets rely on several engineering judgments to implement properly. Sensitivity analysis increases the chances of successful design by exploring the potential changes in conclusions that may result from changes in assumptions and may also identify data collection needs required to reduce uncertainty in the conclusions. In general, sensitivity analysis enables the preparation of more robust water budgets on which to base design recommendations (Mccuen *et al.*, 2002).

Schmidt, (2000) stated that the sensitivity measure proposed by Nearing et al. (1990) is based on the deterministic sensitivity concept formulated by McCuen (1973). The measure was used in this research and defined by the following expression.

$$Sen = \frac{(Y2 - Y1)}{\bar{Y}} \Big/ \frac{(X2 - X1)}{\bar{X}} \qquad Eq\ 3\text{-}22$$

where X1 and X2 are the least and greatest values of input used, $\bar{X}$ is the average of X1 and X2, Y1 and Y2 are the corresponding outputs for the two input values, and $\bar{Y}$ is the average of the two outputs. The parameter Sen is a function of the chosen input range for nonlinear response (Shen *et al.*, 2009), (Schmidt, 2000).

Coefficient of Determination (R^2)

The coefficient of determination is the square of the Pearson's product-moment correlation coefficient and describes the proportion of the total variance in the observed data that can be explained by the model (Legates and McCabe, 1999).

The R^2 assesses the goodness of fit of the linear model by measuring the proportion of variation in y, which is accounted for by the linear model (Tatiana and José, 2021).

It ranges from 0.0 to 1.0, with higher values indicating better agreement, and is given by

$$R^2 = \left\{ \frac{\sum_{i=1}^{n}(O_i - \bar{O})(P_i - \bar{P})}{[\sum_{i=1}^{n}(O_i - \bar{O})^2]^{0.5}[\sum_{i=1}^{n}(P_i - \bar{P})^2]^{0.5}} \right\} \qquad \textit{Eq 3-23}$$

Where the overbar denotes the mean for the entire period of the evaluation. This over-sensitivity to outliers leads to a bias toward the extreme events if correlation-based measures are employed in model evaluation (Legates and McCabe, 1999).

Coefficient of Efficiency (E)

The coefficient of efficiency E has been widely used to evaluate the performance of hydrological models. Nash & Sutcliffe [1970] defined the efficiency coefficient as ranging from minus infinity to 1.0, with higher values indicating better agreement, such as.

$$E = 1.0 - \frac{\sum_{i=1}^{n}(O_i - P_i)^2}{\sum_{i=1}^{n}(O_i - \bar{O})^2} \qquad \textit{Eq 3-24}$$

Physically, E is the ratio of the mean square error.

Thus, a value of zero for the coefficient of efficiency indicates that the observed mean 0 is as good a predictor as the model, while negative values indicate that the observed mean is a better predictor than the model.

The coefficient of efficiency represents an improvement over the coefficient of determination for model evaluation purposes in that it is sensitive to differences in the observed and model-simulated means and variances (Legates and McCabe, 1999).

Index of Agreement (d)

Used to overcome the insensitivity of correlation-based measures to differences in the observed and model-simulated means and variances by developing the index of agreement d, given by early sensitivity to extreme values, as is R^2.

$$d = 1.0 - \frac{\sum_{i=1}^{n}(O_i - P_i)^2}{\sum_{i=1}^{n}(|P_i - \bar{O}| + |O_i - \bar{O}|)^2} \qquad \textit{Eq 3-25}$$

The index of agreement varies from 0.0 to 1.0 with higher values indicating better agreement between the model and observations similar to the interpretation of the coefficient of determination (Legates and McCabe, 1999).

4 RESULTS AND DISCUSSIONS

4.1 Sediment Yield Measurement

4.1.1 Rainfall Distribution

The rainfall distribution of the watershed is known for its variable, short duration, and erratic behavior. It is a unimodal rainfall season that extends from June to September. Most of the time it comes very late and set out early. The rainfall distribution of the modeling years was very variable as always. It was seen starting from the annual rainfall amount for the three consecutive years of modeling which are recorded from a manual rain gauge installed inside the watershed as 737.7, 474, 825.9 mm for 2018, 2019, and 2020, respectively.

The daily maximum rainfall amount and intensity variation caused difficulties in fitting the runoff discharge and especially the runoff peak discharge estimation model for the calibration and validation years. values 41.5, 46.5, and 55 mm are the maximum daily rainfall records for the years 2018, 2019, and 2020, respectively. The duration of rainfall extended from the shortest couple of minutes a day to the longest 6 hrs. a day of rainfall.

The annual rainfall distribution and rainfall intensity of the three consecutive years are illustrated in graphs as shown in (Figure 4-1).

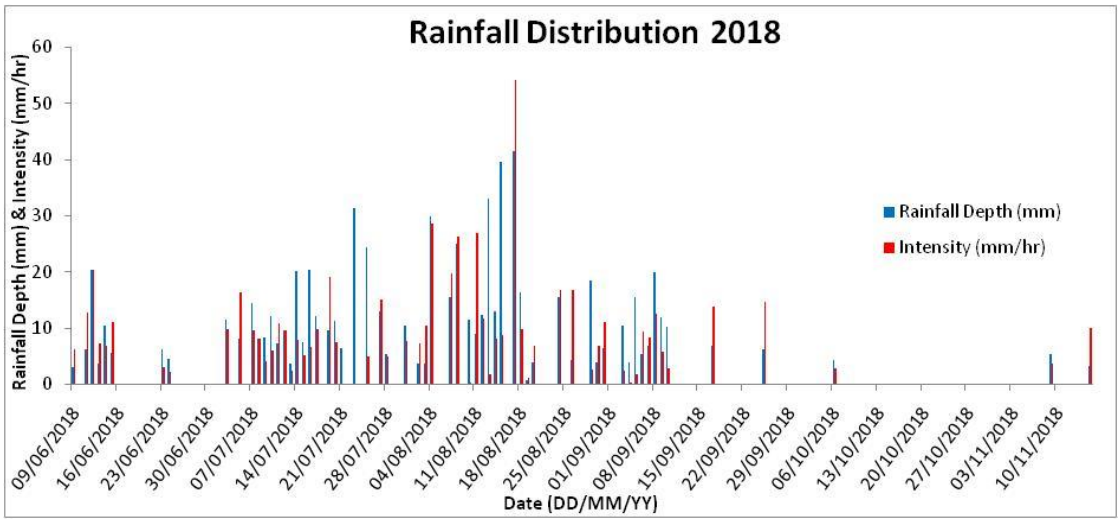

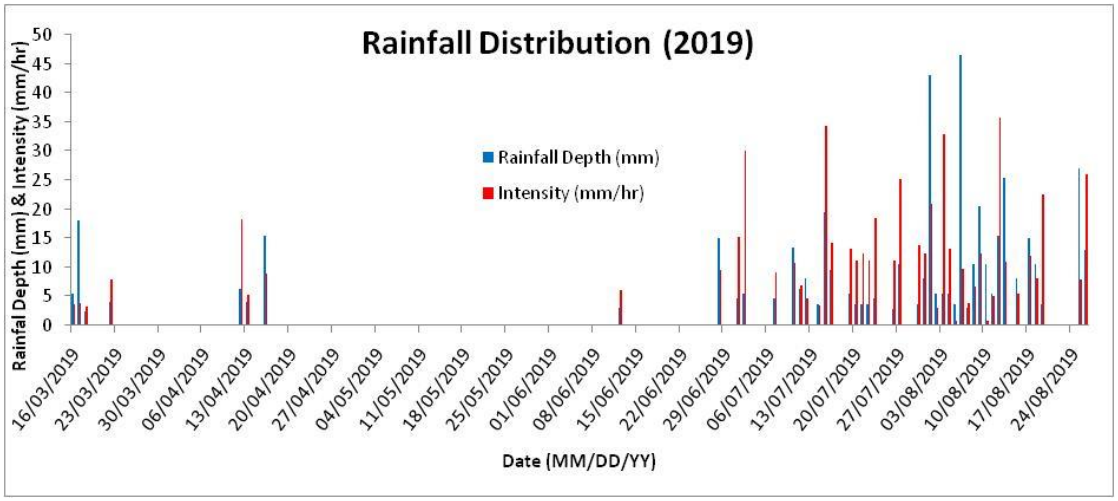

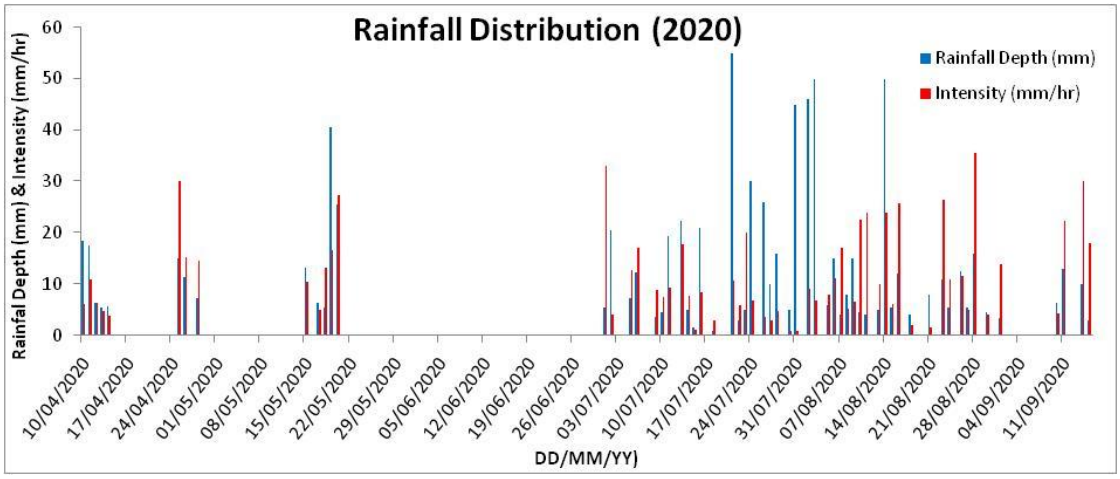

Figure 4-1 Rainfall Distribution (2018, 2019, 2020).

Based on Weibull's method; the data analysis result, 50 mm was the two-year average return period design rainfall.

4.1.2 Sediment Yield Measurement

The sum of sediment yield for observation events was 4.3 t ha^{-1} for 2018, 4.9 t ha^{-1} for 2019, and 12.5 t ha^{-1} for 2020, which has an average value very close to the Maybar condition; as Guzman et al., (2013) reported as mean annual sediment yield estimates of 5.2 t ha−1 yr−1 for Andit Tid, 24.7 t ha−1 yr−1 for Anjeni, and 7.4 t ha−1 yr−1 for Maybar.

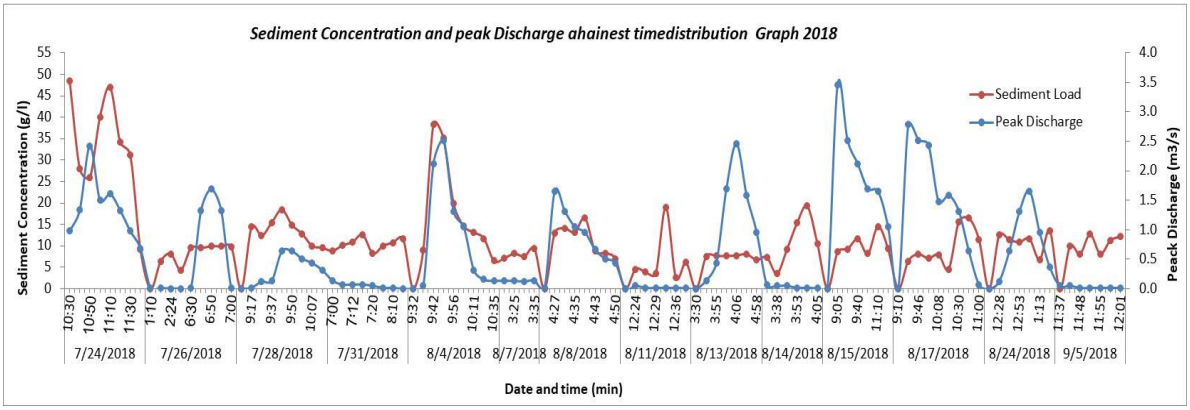

Figure 4-2 Peak Discharge and Suspended Sediment Concentration graph

The graph (Figure 4-2) shows the relation between sediment concentration and runoff peak discharge. The trend of sediment concentration for the runoff events in the first half of the rain season starts high in the beginning and drops down to the end of the runoff event. In the second half of the rainfall season, the sediment concentration of each runoff event tends to stay constant and flat from the beginning to the end of the runoff event. And again, the graphs for the first half of the rain season show, that the sediment concentration graph is most of the time at the top of the peak discharge graph while for the second half it switches to the bottom and the peak discharge graph comes to the bottom.

This shows the response of the sediment concentration to the change in the soil resistance and covers change conditions from the start to the end of the rain season. It is very related to the time series soil resistance and cover condition.

4.1.3 Runoff Stage Discharge Rating Curve and Sediment Rating Curves

Ndomba *et al.*, (2008) suggested that an excellent rating curve could be developed from one hydrological year sediment sampling program data. From the measured runoff depth, discharge, and sediment load, a stage-discharge and Sediment load rating curves, and formulas were developed using a log-log graph.

Using the measured runoff depth runoff velocity and discharge records of 2018, a stage-discharge rating curve is developed as shown in (Figure 4-3), and formula is developed using a log-log graph to make a linear relation.

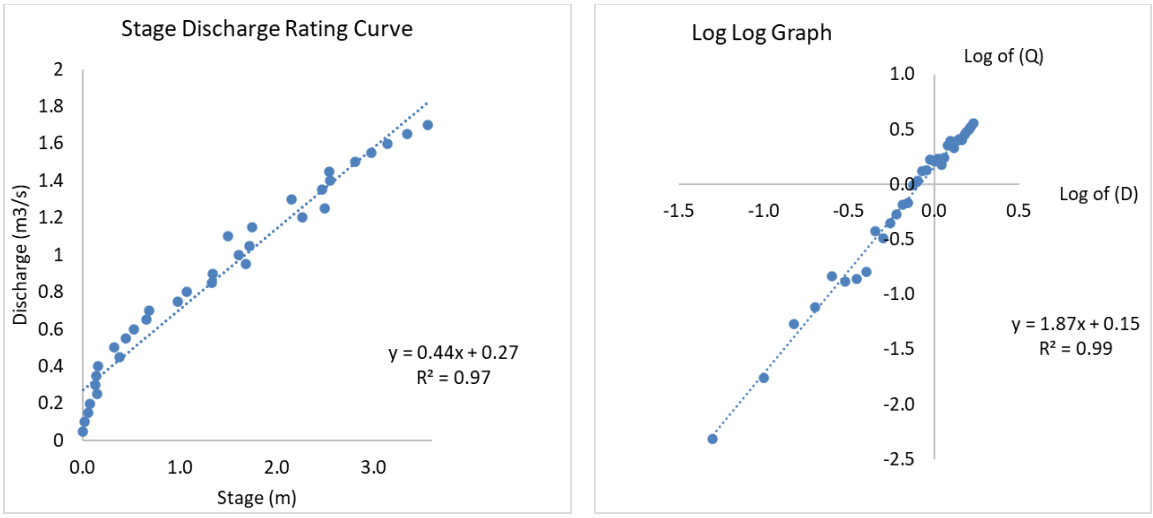

Figure 4-3 Runoff Stage Discharge Rating Curve

A stage-discharge relation formula is commonly written in the form of

$$Q = aD^b$$

Where Q = Discharge, D = Stage, and a and b are coefficients. From the log-log graph, an appropriate stage-discharge rating curve formula was derived as follows.

$$LogQ = b * LogD + loga$$

$$LogQ = 1.87 * x + 0.15$$

$$a = log_{10}0.15 = 10^{0.15} = 1.41$$

$$Q = 1.42D^{1.87} \qquad \textbf{Eq 4-1}$$

According to different literature, the sediment rating curve formula has the same form as the stage-discharge rating curve. Based on the 2018 measured discharge and sediment load data a scattered plot is shown below in (Figure 4-4).

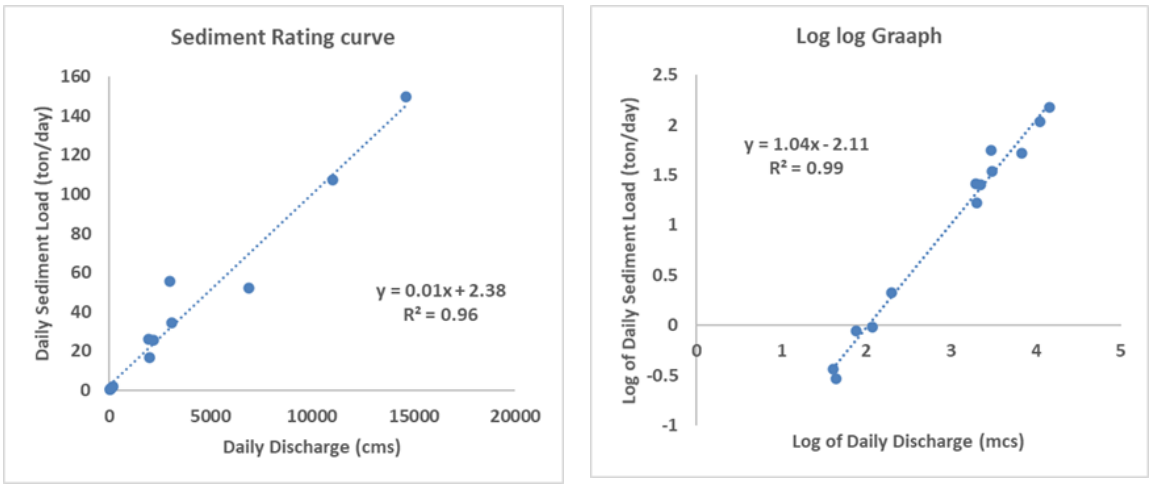

Figure 4-4 Suspended sediment load rating curve

The suspended sediment load rating curve formula for Agewmariam watershed will be

$$L = aL^{b}$$

$$Log\ L = b * LogQ + loga$$
$$Log\ L = 1.04 * Log\ Q + Log\ -2.11$$

$$L = 0.01Q^{1.04} \qquad \textbf{Eq 4-2}$$

In doing so a good rating curve with a high coefficient of determination (R^2) of 0.99 for both curves were found and the formulas are rewritten to their most preferred form. These rating curve formulas were used to calculate discharge and can facilitate the modeling process thorough filling the gap in the data provided to the model by interpolation and extrapolation.

4.2 MUSLE Model Simulation of Sediment Yield

For the application of the MUSLE model in the prediction of soil loss in Agewmariam watershed the five factors, namely the runoff energy factor, soil erodibility factor, slope length & steepness factor, cover factor, and support practice factor are analyzed and processed to give their respective representative values and some values adopted.

4.2.1 Runoff Energy Factor Result

For the determination of the most variable factor; the runoff energy factor; 13 storm events from the 2018 rain season for calibration and 14 storm events from the 2019 and 2020 rain for validation were screened based on the quality of the data by rejecting some outliers.

The average curve number (CN) value of the watershed is determined based on the soil hydrologic group (SHG), the land use type, and the slope of the watershed. The soil texture classes found in the watershed can be related to only soil hydrologic groups A, B, and C based on (Appendix table 3).

The curve number values were assigned for each land use, hydrologic soil group, antecedent soil moisture condition, and slope condition as shown in (Table 4-1). The watershed average curve number value was found to be 56.4 for AMC II and adjusted into 32.1 and 74.4 for AMC I and AMC II respectively. These values are then adjusted for the corresponding land slope and found to an average curve number value of 59.9 which is a very reasonable result relative to the calibrated curve number value of 61.77.

Table 4-1 Curve Number Value in the Watershed

No	Land use/ SHG	Area (ha)	SHG	CN AMC I	CN AMC II	CN AMC III	Slope Adjusted CN	Calibrated CN
1	Cultivation Land	84.49	A	38.7	59	77.1	61.1	
2	Bare Land	2.29	A	59.5	77	88.7	80.4	
3	Bush Land	11.01	A	15.8	30	50.1	36.6	
4	Scattered Bush	37.96	A	28.8	48	68.4	54.6	
5	Settlement	4.40	A	38.7	59	77.1	62.7	

6	Cultivation Land	1.13	B	50.6	70	84.5	71.6	
7	Bare Land	0.13	B	72.9	86	93.5	88.2	
8	Cultivation Land	12.80	C	60.9	78	89.3	79.3	
9	Bare Land	0.66	C	81.6	91	95.9	92.4	
10	Bush Land	0.13	C	28.8	48	68.4	54.7	
11	Scattered Bush	0.37	C	59.5	77	88.7	80.8	
12	Settlement	0.026	C	66.6	82	91.4	84.0	
13	Bush Land	0.00001	A	15.8	30	50.1	36.6	
14	Scattered Bush	0.00001	A	28.8	48	68.4	54.7	
	Wt. Ave. CN			37.1	56.4	74.4	59.9	61.77

Source: (Cronshey *et al.*, 1986), (Boonstra, 1994), (Mishra and Singh, 2003), (Chow *et al.*, 1988), (Valentina and Frank, 2000).

An estimation of the runoff depth from an estimated curve number value of AMC III of 74.4, and an adopted initial abstraction to Storage ratio of 0.2 from the origin of the formula by Cronshey *et al.*, (1986); exaggerated the result as compared to the observed value; even not satisfying the precondition set as runoff starts as initial abstraction gets less than or equal to precipitation.

One reason is that the SCS developers assumed that the initial abstraction to storage ratio ($\boldsymbol{\lambda}$) is equal to 0.2 which is not true in Agewmariam watershed condition in reality which is 0.023 based on the smallest observed runoff event in the model run period; so that, we had to adjust the curve number value for the slope condition in the watershed and to fit the observed values.

In line with our result; different researchers reviewed the value of the initial abstraction to storage ratio ($\boldsymbol{\lambda}$) and suggested adjusting it based on the local condition of use. They found a good result by reducing it from its original value of 0.2 to 0.05 for the SWB version 2 model use; Westenbroek *et al.*, (2018), to 0.03 for the Indian condition by Satheeshkumar *et al.*, (2017), to 0.014 for Greece & Czech Republic, according to Baltas *et al.*, (2007), by Caletka *et al.*, (2020), and finally to 0.01 for the conditions of Ethiopian highlands according to Assaye *et al.*, (2021).

The second reason is in line with the conclusion of Stone et al., (2000); it is because the Curve Number is a storm total rainfall-runoff relationship, that does not account for variability in rainfall intensity which, in semiarid regions, can be a dominant factor in the runoff amount produced.

Using an adjusted value of initial abstraction to storage ratio (λ) of 0.023 and calibrated curve number value of 61.77 the runoff depth was estimated with the best value to fit the observed value as shown in (Table 4-2) & (Table 4-8).

Table 4-2 Observed and Estimated Runoff Discharge Comparison Table

No	Date	P (mm)	Estimated Discharge		Observed Discharge
			Depth (mm)	Volume (m3)	(m3)
1	7/26/2018	24.5	2.55	3489.3	1989.6
2	7/28/2018	13	0.65	721.9	1936.3
3	7/31/2018	10.5	0.40	384.0	200.5
4	8/4/2018	30	3.84	5446.3	2984.1
5	8/7/2018	15.5	0.97	1158.7	118.7
6	8/8/2018	25	2.66	3651.3	2199.3
7	8/11/2018	9	0.27	230.5	43.8
8	8/13/2018	33	4.63	6669.0	6859.1
9	8/14/2018	13	0.65	721.9	75.3
10	8/15/2018	39.5	6.56	9666.4	14601.8
11	8/17/2018	41.5	7.21	10679.2	11010.6
12	8/24/2018	15.5	0.97	1158.7	3076.2
13	9/5/2018	15.5	0.97	1158.7	40.7

It can be seen from the result that still; the effect of rainfall variability remains hidden causing an error in the discharge estimation. The discharge is attributed to the rainfall intensity as much as it is attributed to the rainfall amount. The result from the table confirms that; coming up with the largest rainfall amount sometimes results in smaller runoff depth or vice versa. And also, sometimes similar rainfall amounts result in different runoff depths. This indicates the presence of a rainfall intensity effect.

For the estimation of peak discharge, it could have been used the rational formula for estimating peak discharge of runoff from a catchment using rainfall intensity for the selected

period, runoff coefficient, and catchment area (Shilton et al., 2015); But it has limitations, as it is suggested for estimating peak flows for drainage areas up to 80 hectares (200 acres) in size, and Use of the rational formula on larger drainage areas above this limit requires the use of sound engineering judgment to ensure that reasonable results are obtained (PennDOT, 2015).

To estimate the peak discharge using the SCS graphical peak discharge method estimation of the unit peak discharge for the site was a prerequisite. For the unit peak discharge to be estimated the time of concentration was calculated and found to be 0.22 for the sheet flow, 0.275 for the concentrated shallow flow, and 0.166 for the channel flow with a total of 0.661 hrs. using (Eq 3-13) of the SCS velocity method.

Based on the (Eq 3-17); using the calculated time of concentration and the regression coefficients set by SCS/NRCS for a type II design storm curve as shown in (Appendix table 4); the most sensitive value so-called unit peak discharge is found to be 0.00196 m^3/s/ha/mm; which is very different from the calibrated value of 0.00334 m^3/s/ha/mm. Similar to different authors' disproval of the direct use of the SCS-developed type II design storm curve; it is not appropriate to use for the watershed condition. Even the calibrated unit peak discharge of 0.00334 m3/s/ha/mm needs further improvement using more data.

Using the calibrated value of unit peak discharge, the peak discharge for each storm event was estimated as shown in (Table 4-3) and (Table 4-8).

Table 4-3 Observed and Estimated Runoff Peak Discharge Comparison Table

No	Date	P (mm)	Estimated Peak Discharge (m3/s)	Observed Peak Discharge (m3/s)
1	7/26/2018	24.5	1.34	1.69
2	7/28/2018	13	0.28	0.64
3	7/31/2018	10.5	0.15	0.14
4	8/4/2018	30	2.09	2.51
5	8/7/2018	15.5	0.44	0.14

6	8/8/2018	25	1.40	1.66
7	8/11/2018	9	0.09	0.05
8	8/13/2018	33	2.56	2.46
9	8/14/2018	13	0.28	0.07
10	8/15/2018	39.5	3.71	3.45
11	8/17/2018	41.5	4.09	2.78
12	8/24/2018	15.5	0.44	1.66
13	9/5/2018	15.5	0.44	0.05

From the result table, it can be realized that the effect of rainfall intensity affects the peak discharge the same way it affected the runoff depth, even a fold. The rainfall distribution variability influences the peak discharge estimation accuracy twice; once in the runoff depth estimation and second in the unit peak discharge estimation.

4.2.2 Soil Erodibility Factor (K) Result

In general soil erodibility, is a function of the Soil's infiltration capacity, hydraulic conductivity, water storage capacity, particle dispersion, detachability, abrasion, and mobility by rainfall and runoff; although they are related in one way or another. Of the total 155 soil samples collected from the entire watershed, five textural classes; such as Sandy Loam, Sandy Clay Loam, Loam, Loamy Sand & Sand, and an organic carbon content ranging from 0.02 to 3.18 % were identified.

From the above available data, the soil erodibility factor is calculated by using (Eq 3-19) on an Excel sheet and interpolated on the ArcGIS environment using the ordinary kriging technique. Based on the calculation, the soil erodibility factor value ranged from 0.12 to 0.237; which is in between the formula range set by the developers to vary from 0.1 to 0.5 Mg ha^{-1} MJ^{-1} mm^{-1} (Sharpley and Williams, 1990).

This value is higher than the value determined by Girmay *et al*., (2020) for the same watershed using different formulas and input to use in the application of the USLE model, which ranges from 0.079 to 0.173. The formula used for soil erodibility factor (K)

determination is used for its advantage in permitting soil erodibility factor calculation in the absence of soil permeability and structure data. But it has a limitation that restricts the result to lay in between 0.1 and 0.5 while other literature justifies as it can spread further from 0 to o.7 (Pandey *et al.*, 2021).

As illustrated in (Figure 4-5) The highest erodibility factor value is found on the upper north western part of the watershed which means the most susceptible soil to erosion and that area is characterized by low organic matter content and more fine soil particles; easy to detach and transported by water. It decreases down to the southeast side of the watershed and reaches the minimum value k on the eastern side of the watershed which is characterized by more sand-sized soil particles that are not easy to transport and generate runoff.

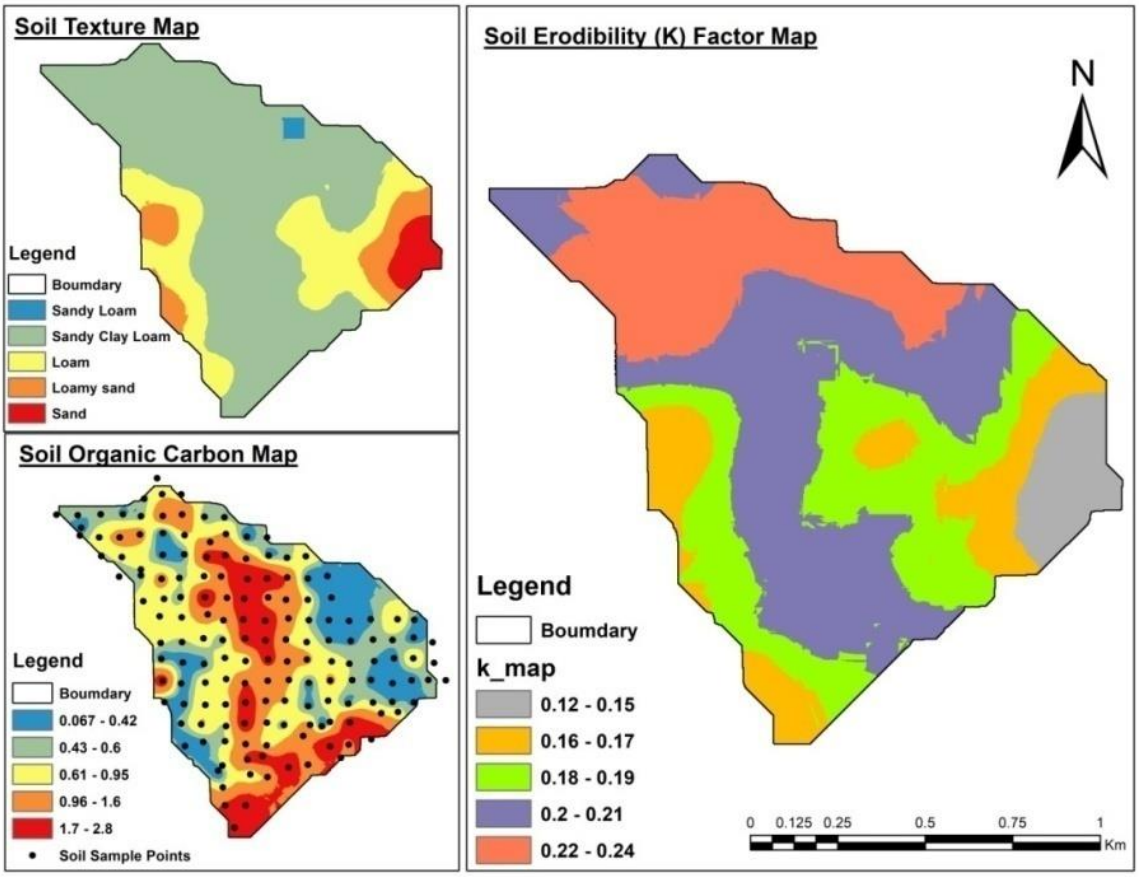

Figure 4-5 Soil Erodibility Factor (K) Map

4.2.3 The Slope Length & steepness Factor (LS) Result

Hrabalíková and Janeček, (2017) confirmed that the best method for LS factor estimation on a field scale is the original manual method of the USLE, which is the one used in this research.

The slope length & steepness factor is calculated using (Eq 3-20) or (Eq 3-21) from a 2m resolution DEM which resulted in better detail to represent the area since the area is characterized by high variability of the slope within a small distance. The high-resolution DEM improved the quality of the analysis by catching variability within a 2 m difference. In line with Bircher *et al.*, (2019) the very fine resolution DEM reduced the edge effect during watershed delineation, and differentiated soil erosion risk depressions reliably to better represent the reality. It brought improvements starting from the delineation of the watershed on Arc SWAT by increasing the area from 147 ha to 155.39 ha and by following the actual groundwater divide line; as compared to the 30m DEM resolution.

To calculate the LS factor; the values of m in the equation were determined by classifying the slope of the watershed into the predefined classes (Wischmeier and Smith, 1978) as shown in (Appendix table 7); in which 95 % is found to be in a class > 5 % in consequence, a fixed 0.5 value of m. The LS factor varied within a range of 0 to 791. The values that cover most of the area are below 50 except for the small portion of the watershed encountered with the highest extreme values around hill slope areas and following the natural streamline, which is characterized by high slope change. Out of the 155.3 ha watershed area, 72.2 % has an LS factor value less than 20; 24 % have an LS value between 20 and 50, 3.3 % have an LS value between 50 and 100, and only the rest 0.5 % of the total watershed area encountered the highest extreme LS factor value extending from 51 to 791.

Table 4-4 Slop Length & steepness Factor Coverage

No	LS Value Range	Area	% Coverage
1	< 20	112.2	72.2
2	20-50	37.2	24.0
3	50-100	5.2	3.3
4	100-150	0.6	0.4
5	> 150	0.2	0.1
	Total	155.4	100

It is obvious that as can be seen from the value it contributes to the soil loss equation; the slope length & steepness factor is with the greatest influence. In line with this result, different authors have confirmed that the slope length & steepness factor is the largest contributing factor to soil loss (Panagos *et al.*, 2015); (Girmay *et al.*, 2020). This is because the LS factor is the most sensitive parameter in the soil loss prediction models.

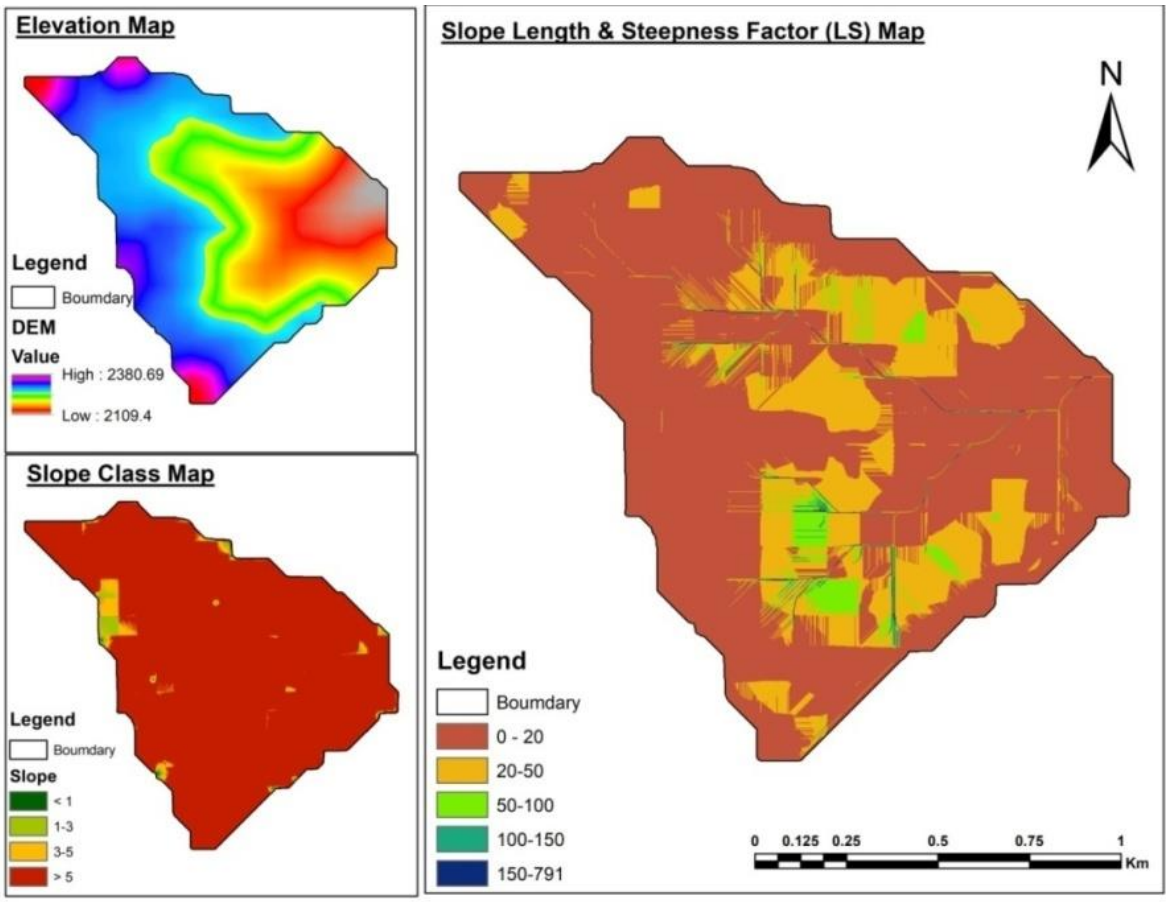

Figure 4-6 Slope Length & steepness Factor Map

4.2.4 Cover Factor (C) Result

For the determination of the cover factor and support practice factor value, the land use land cover type of the area was identified by the ground survey and digitized on Google earth pro. The area is characterized by five major land use/land cover practices as listed in (Table 4-5) and terracing as a major support practice activity. The values for each land use land cover type are adopted from Hurni, (1985), Girmay *et al.*, (2020), and Wischmeier and Smith, (1978), as shown in (Appendix table 8) for each crop type.

The bare land on the upper south and middle part of the watershed is with the highest cover factor value of 1; which means very prone to erosion. The cultivation land that is the highest in area coverage has a value of 0.15 for cereals and pulses, 0.1 for sorghum, and 0.25 for linseed (Hurni, 1985). For the rest of the scattered bush and dense bushlands; a cover factor value of 0.14 and 0.012 is assigned respectively according to Wischmeier and Smith, (1978); which means they are more protected and less prone to erosion.

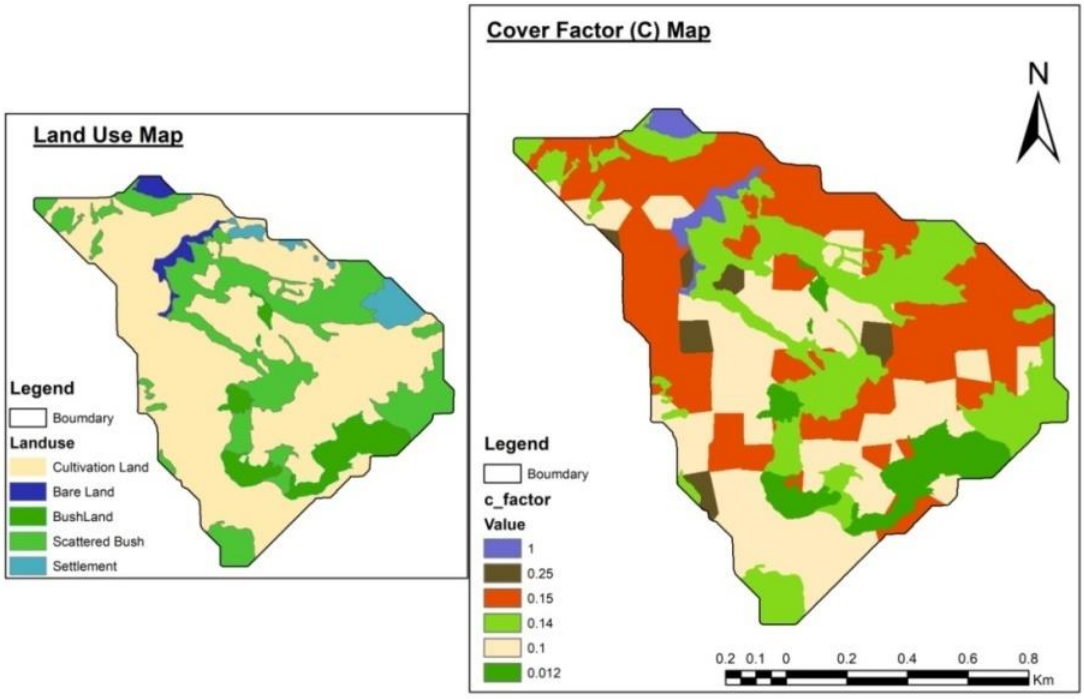

Figure 4-7 Cover Factor (C)Map

The land-use type distribution percent coverage is shown below in (Table 4-5). The majority of the watershed area is covered by cultivation land and scattered bushland which covers 88 % of the total watershed area.

Table 4-5 Land Use Type Coverage Based on Slope.

No	Land use/ Land cover	Area (ha)	% Cover
1	Cultivation Land	98.42	63.3
2	Bare Land	3.08	2.0
3	Dense bush	11.13	7.2
4	Scattered Bush	38.34	24.7
5	Settlement	4.42	2.8
	Total	155.39	100

4.2.5 Support Practice Factor (P) Result

The support practice factor is determined from the surface map of the land use type and the slope map of the watershed. For the bushland, scattered bush, and settlement area a value of 1and 0.8 is assigned considering the areas with little or no support practice factor (Girmay, *et al.*, 2020), (Benavidez *et al.*, 2018). For the cultivation land use areas, the watershed is divided into five classes based on slope and a value assigned for each class according to (Shin, 1999) for the terracing support practice.

Figure 4-8 Terracing Practice in the Watershed

As shown in the figure, the highest values of support practice factors are observed in the middle parts of the watershed following the bushlands and the steep slope cultivation lands.

The lowest values are observed on the upper and bottom parts of the watershed following the flat slope cultivation lands with a terracing practice.

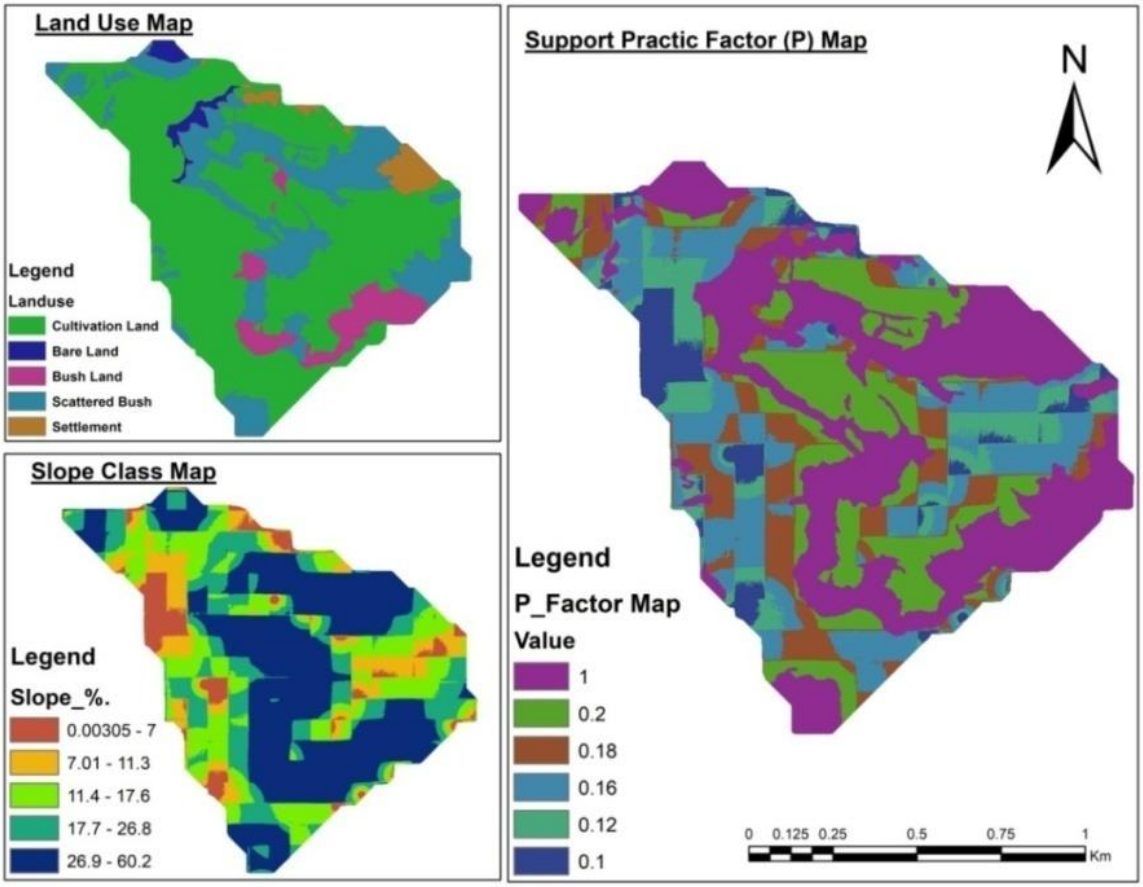

Figure 4-9 Support Practice Factor (P) Map

4.3 Sediment Yield and Model Evaluation

4.3.1 Parameter Sensitivity Analysis

For the MUSLE model, a parameter sensitivity analysis was performed to identify the most important parameters of the model and is carried out based on changes to the objective function depending on the interactions among parameter values. Then, a linear approximation of the model parameters is made in agreement with the sensitivity of the objective function.

The results of the parameter sensitivity analysis for nine parameters; come up with an order of curve number, slope length and steepness factor, energy factor exponent, support practice factor, unit peak discharge, soil erodibility factor, cover management factor, energy factor coefficient, and initial abstraction to storage ratio; from the highest to the least influencing parameter.

No	Parameter	Sensitivity
1	Initial abstraction to storage ratio (λ)	-0.04
2	Curve number (CN)	3.00
3	Unit peak discharge (qu)	0.74
4	Energy factor coefficient (a)	0.16
5	Energy factor exponent (b)	1.29
6	Soil erodibility factor (K)	0.64
7	Slope length & steepness factor (LS)	1.57
8	Cover management factor (C)	0.26
9	Support practice factor (P)	0.86

In line with others Stone et al., (2000) the curve number is a highly sensitive parameter. From this, it is possible to conclude that the runoff energy factor is the most sensitive parameter.

Arnold et al., (2012) concluded that the sensitivity of one parameter often depends on the value of other related parameters; hence, the problem with the one-at-a-time analysis. It was unexpected for the initial abstraction to storage ratio to have the least sensitivity value unless it had the smallest range of input values for the parameter sensitivity analysis. So, looking over another method of sensitivity analysis will have a better result in a sensitivity evaluation.

The results of the parameter sensitivity analysis for nine parameters are provided in the chart below in figure (Figure 4-10).

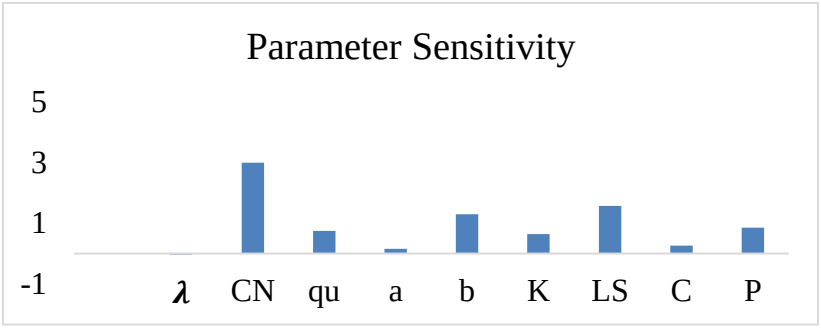

Figure 4-10 Model parameter sensitivity analysis chart.

Next to the runoff energy factor, the slop length & steepness factor is with the highest sensitivity value. This is in line with the conclusion made by (Panagos *et al*., 2015), (Girmay *et al.*, 2020), etc.

4.3.2 Sediment yield for the Calibration Period

The estimated sediment yields and the observed sediment yields were compared against each other as shown below in (Table 4-6). The model has tended to come up with a little exaggeration of the overall value of sediment yield as compared to the observed sediment yield. The variation has resulted from the high variable trend of the temporal rainfall intensity distribution in the area.

Table 4-6 Observed and Estimated Sediment Loss Comparison Table

No	Date	P (mm)	Estimated Sediment Loss (ton/ha)	Observed Sediment Loss (ton/ha)
1	7/26/2018	24.5	0.214	0.108
2	7/28/2018	13	0.033	0.168
3	7/31/2018	10.5	0.016	0.014
4	8/4/2018	30	0.361	0.356
5	8/7/2018	15.5	0.058	0.006
6	8/8/2018	25	0.226	0.164
7	8/11/2018	9	0.009	0.002
8	8/13/2018	33	0.458	0.334
9	8/14/2018	13	0.033	0.006
10	8/15/2018	39.5	0.710	0.963
11	8/17/2018	41.5	0.798	0.689
12	8/24/2018	15.5	0.058	0.221
13	9/5/2018	15.5	0.058	0.002

For the calibration period, the event-based mean observed and estimated suspended sediment yields can be summarized as 0.2 and 0.23 ton/ha respectively.

From the graph here it is possible to see the sediment yield is very related to the rainfall distribution, the runoff discharge, and the peak discharge. Some simulations of two runoff events with the same amount of rainfall come up with different sediment yield measured values but with the same sediment yield prediction value. So, it shows that the rainfall intensity still affects the sediment yield prediction accuracy.

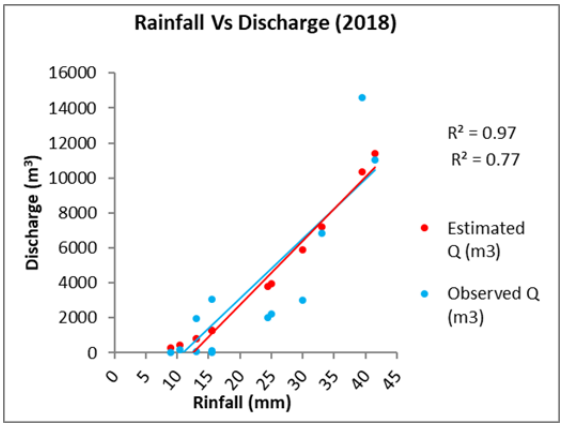

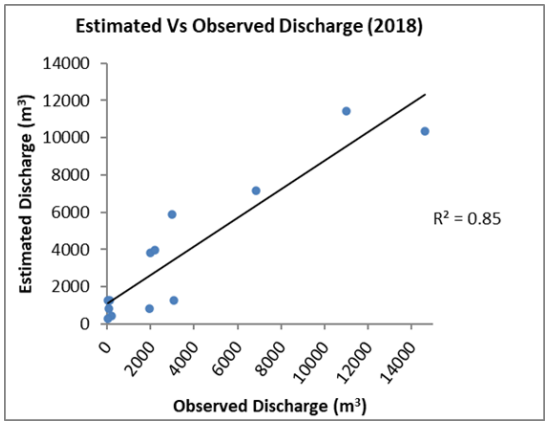

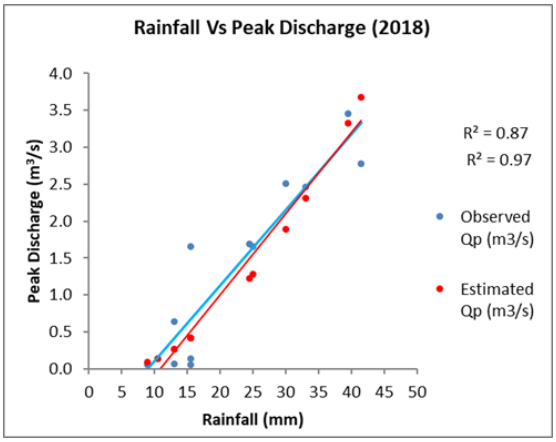

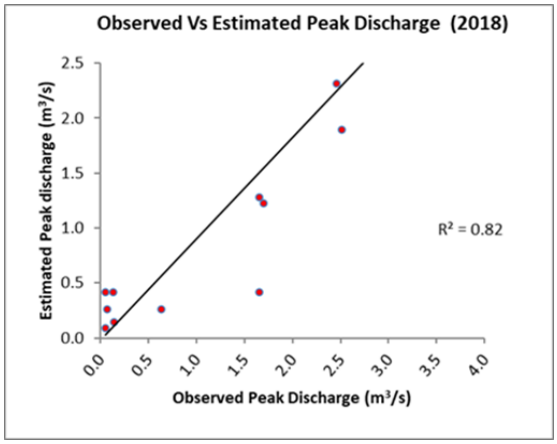

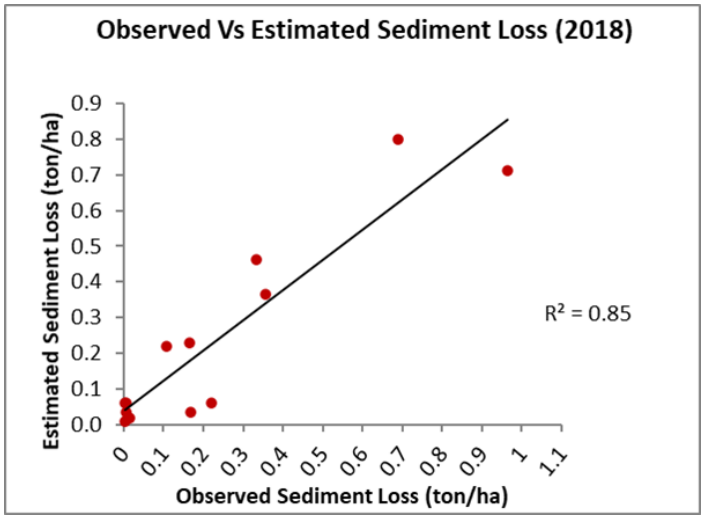

Figure 4-11 Rainfall, Estimated Vs. Observed Runoff discharge, Peak Discharge, and Sediment Load Graph for the Calibration Period

For the calibration period, the overall model evaluation criteria show a good fit between the observed and model estimated values as shown in (Table 4-7).

Table 4-7 Model Evaluation Summary for the Calibration Period

Validation Period	**Modeling**		
Evaluation Criteria	**Runoff Discharge**	**Peak Discharge**	**Sediment Loss**
Coefficient of Determination (R^2)	0.85	0.82	0.85
Coefficient of Efficiency (E)	0.84	0.8	0.85
Index of Agreement (D)	0.95	0.95	0.96

The sediment yield prediction accuracy evaluation has come up with a Coefficient of Determination (R^2) of 0.85, a Coefficient of Efficiency (E) of 0.85, and an Index of Agreement (D) of 0.96 which can be rated as a very good model performance according to Moriasi et al., (2015).

4.3.3 Sediment yield for the validation period

For the validation period the observed and estimated runoff discharge, runoff peak discharge, and sediment yield are illustrated in (Table 4-8) for comparison. The model has tended to come up with a little underestimation of the overall value of sediment yield simulation.

Table 4-8 Discharge Volume, Peak Discharge, and Sediment Loss for the Validation Period

No	Date	P (mm)	Estimated Discharge		Observed Discharge (m^3)	Estimated Peak Discharge (m^3/s)	Observed Peak Discharge (m^3/s)	Estimated Sediment Loss (ton/ha)	Observed Sediment Loss (ton/ha)
			Depth (mm)	Volume (m^3)					
1	7/15/2019	19.5	1.6	2053.2	500.1	0.787	0.737	0.11	0.11
2	7/19/2019	5.5	0.1	22.4	290.0	0.009	0.172	0.0008	0.02
3	8/1/2019	43	7.7	11465.3	9682.4	4.396	2.690	0.87	1.18
4	8/6/2019	46.5	8.9	13385.4	21108.2	5.132	3.909	1.04	2.58
5	8/9/2019	20.5	1.8	2313.0	3664.3	0.887	2.204	0.13	0.34
6	5/17/2020	6.4	0.1	55.4	20.8	0.021	0.016	0.0021	0.0019
7	7/13/2020	22.3	2.1	2815.5	69.9	1.079	0.060	0.17	0.02
8	7/24/2020	30	3.8	5446.3	321.3	2.088	0.135	0.36	0.04
9	7/26/2020	26	2.9	3985.1	434.0	1.528	0.158	0.25	0.04
10	7/31/2020	45	8.4	12548.0	7021.8	4.811	2.460	0.96	1.59
11	8/2/2020	46	8.8	13103.9	9414.8	5.024	1.486	1.02	1.21
12	8/3/2020	50	10.2	15420.6	15918.7	5.912	1.078	1.23	1.67
13	8/14/2020	50	10.2	15420.6	13405.6	5.912	4.969	1.23	1.63
14	8/28/2020	16	1.0	1257.6	135.9	0.482	0.258	0.06	0.01

For the validation period, the event-based mean observed and estimated suspended sediment yields were 0.7 and 0.53 ton/ha respectively.

The runoff peak discharge modeling has contributed to the great exaggeration even to an unacceptable level leading to a conclusion to substitute the graphical peak discharge estimation method. The variation has resulted from the high variable trend of temporal rainfall intensity distribution and the lack of the graphical peak discharge estimation method to address the good representation of the rainfall distribution type in the area. It is because the peak discharge estimation is attributed to the effect of rainfall distribution twice; once in the runoff depth estimation and second during the estimation of the unit peak discharge.

The peak discharge estimation shows the lowest evaluation value which has caused the final result as a whole to bias as compared to the calibration period.

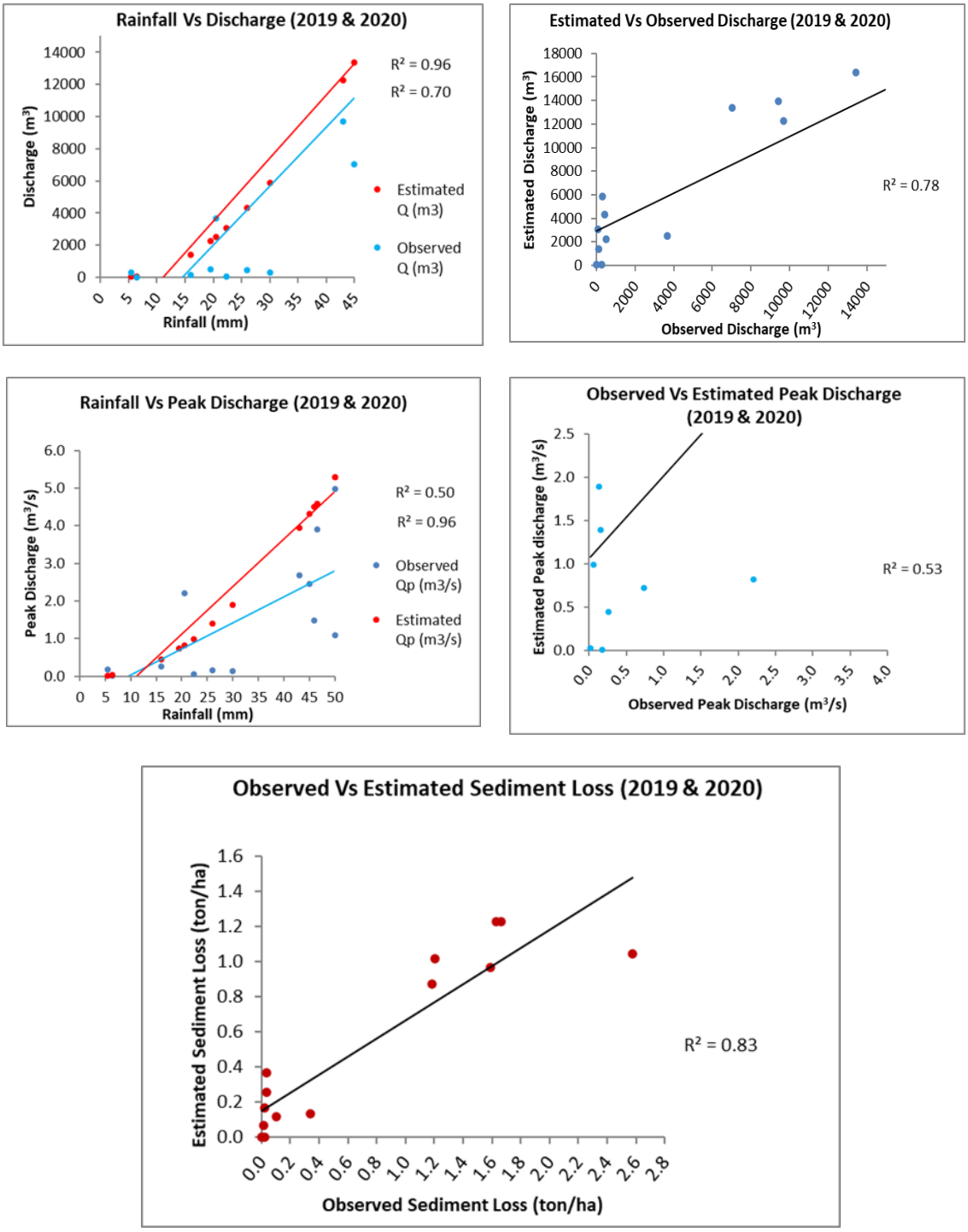

Figure 4-12 Rainfall, Estimated Vs. Observed Runoff discharge, Peak Discharge, and Sediment Load Graph for the Validation Period

For the validation period also, the model evaluation shows a good fit between the measured and model estimated values but, as compared to the calibration period, the coefficient of determination shows some bias, especially for the peak discharge modeling. This is because

the rainfall distribution of the validation period varies widely as compared to the rainfall distribution of the calibration period.

Table 4-9 Model Evaluation Summary for the Validation Period

Validation Period	Modeling		
Evaluation Criteria	**Runoff Discharge**	**Peak Discharge**	**Sediment Loss**
Coefficient of Determination (R^2)	0.78	0.53	0.84
Coefficient of Efficiency (E)	0.71	0.97	0.65
Index of Agreement (D)	0.91	0.77	0.83

The sediment yield prediction accuracy evaluation has come up with a Coefficient of Determination (R^2) of 0.83, a Coefficient of Efficiency (E) of 0.65, and an Index of Agreement (D) of 0.85 which can be rated as very good and good model performance according to Moriasi et al., (2015). The peak discharge estimation shows the lowest evaluation value.

Finally, the original formula of the MUSLE is expressed as in equation (Eq 3-6) and after the calibration of the runoff energy components relative to the observed data the coefficients that relate the runoff energy factor to the sediment loss rate, are changed and the coefficients of the formula are modified as

$$Y = (Q * qp)^{0.59} KLSCP \qquad \textbf{Eq\_ 4-3}$$

Where: Y = the sediment yield from an individual storm in metric tons, Q = the storm runoff volume in m^3, qp = the peak runoff rate in m^3/sec, K = the soil-erodibility factor, LS = the slope length and gradient factor, C = the crop management factor, and P = the erosion-control-practice factor.

The value of coefficient (a) in the MUSLE formula for the watershed condition is found to be 1 with a tendency to reduce blow 1 whereas the value of exponent (b) is found to be 0.59 with a tendency to increase close to 1. This is in line with the Jackson *et al.*, (1986)

conclusion that the exponent on the formula may be too low for arid and semi-arid rangeland drainage basins, where runoff is mostly from thunderstorms and needs to be recalibrated for these basins using storm period data before average annual sediment yield prediction has merit. Tsige *et al*., (2022) also concluded that the best exponent (b) of the Modified Universal Soil Loss Equation for the Ethiopian condition is 1.

In the worst scenario of evaluation, this calibrated formula (***Eq_ 4-3***) enabled us to estimate soil erosion in Agewmariam watershed with a 0.83 coefficient of determination (R^2), a 0.65 coefficient of efficiency (E), and a 0.85 index of agreement (D) which is considered as a very good model performance.

5 CONCLUSION AND RECOMMENDATION

The result revealed the use of the MUSLE model in its original form without calibration is not proper.

The curve number method finally estimated the runoff discharge almost perfectly. But it needs a proper determination of the value of the curve number and the initial abstraction (Ia) to the storage ratio ($\boldsymbol{\lambda}$) and then; a calibration based on observed data from a field; because there was a great exaggeration of runoff discharge estimation before the calibration is done.

As it has been seen from the modeling result, The peak discharge modeling using the SCS graphical peak discharge estimation method was the most influential part to cause a bias in the sediment modeling process. It has introduced more errors in the model greater than any other factor does. In the estimation of runoff peak discharge, establishing a well-representing rainfall distribution type curve for Ethiopian conditions up to the local stage is recommended. Rather, establishing a methodology that can relate the eventual rainfall intensity to the peak discharge is a better point of view for future improvement.

To recognize and recommend the MUSLE model for further application in sediment yield modeling in the study area; with better accuracy, the graphical peak discharge estimation method has to be substituted with other methods of peak discharge estimation through research. In general, for the hydrologic modeling part, greater numbers of storm events, as well as case studies need to be considered in the future.

The hydrologic modeling parameters were the most sensitive and variable parameters identified based on the sensitivity analysis and observation of data property. The other parameters were considered or remained constant across each modeling event.

Its accuracy can be further improved by using spatially and temporally fine resolution input data from an accurate and available source like google earth and a detailed field survey; bearing in mind its prediction potential to be improved by doing further analysis of other extra quality observed data from the field.

Finally, this study has shown that the model, in general, still with its limitations the model can be used as a good tool for soil and water management and planning activities in Agewmariam. With the existing performance of the model, it can be used for a spatial prioritization in the selection of erosion hotspot areas for immediate action of soil and water conservation and priority should be given to those areas with a highly steep slope and with no cover and support practice. It is possible to extrapolate and use the model for Agewmariam watershed and neighboring similar watersheds as a tool for planning and decision making.

REFERENCE

A. Griensven, T. Meixner, S. Grunwald, T. Bishop, M. Diluzio, and R. Srinivasan., (2006) 'A global sensitivity analysis tool for the parameters of multi-variable catchment models', 324, pp. 10–23. doi: 10.1016/j.jhydrol.2005.09.008.

Adimassu, Z., Langan, S. and Barron, J., (2018). Highlights of soil and water conservation investments in four regions of Ethiopia (Vol. 182). International Water Management Institute (IWMI).

Alberta (2009) water measurement guidebook.

Alemayehu, A.A., Muluneh, A., Moges, A. and Kendie, H., (2020). Estimation of sediment yield and effectiveness of level stone bunds to reduce sediment loss in the Gumara-Maksegnit watershed, Nile Basin, Ethiopia. Journal of Soils and Sediments, 20(10), pp.3756-3768.

Amsalu, T. and Mengaw, A. (2014) 'GIS-Based Soil Loss Estimation Using RUSLE Model: The Case of Jabi Tehinan Woreda', pp. 616–626.

An L.S., Liao, K.H., Zhou, B.H., Pan, W. and Chen, Q., (2016) 'Global sensitivity analysis of the parameters of the modified universal soil loss equation', Applied Ecology and Environmental Research, 14(4), pp. 505–514. doi: 10.15666/aeer/1404_505514.

Andrade, P. and Heun, J. (2011) 'A General Guide to Global Positioning Systems (GPS).

Assaye, H. et al. (2021) 'Curve number calibration for measuring impacts of land management in sub-humid Ethiopia to cite this version: HAL Id: hal-03197727', Journal of Hydrology: Regional Studies, 35, p. 100819. doi: 10.1016/j.ejrh.2021.100819.

Badege, B. (2001) 'Deforestation and Land Degradation in the Ethiopian Highlands: A Strategy for Physical Recovery', Northeast African Studies, 8(1), pp. 7–25. Available at: http://www.jstor.org/stable/41931353.

Balamurugat, G. (1989) 'The Use of Suspended Sediment Rating Curves in Malaysia Some Preliminary Considerations', Pertanika, 12(3), pp. 367–376.

Baltas, E. A., Dervos, N. A. and Mimikou, M. A. (2007) 'Technical note: Determination of the SCS initial abstraction ratio in an experimental watershed in Greece', Hydrology and Earth System Sciences, 11(6), pp. 1825–1829. doi: 10.5194/hess-11-1825-2007.

Bečvář, M. (2006) 'Sediment Load and Suspended Sediment Concentration Prediction', Soil Water Res, 2006(1), pp. 23–31.

Benavidez, R., Jackson, B., Maxwell, D., and Norton, K., (2018). A review of the (Revised) Universal Soil Loss Equation ((R) USLE): With a view to increasing its global applicability and improving soil loss estimates. Hydrology and Earth System Sciences, 22(11), pp.6059-6086.

Bircher, P., Liniger, H.P. and Prasuhn, V., 2019. Comparing different multiple flow algorithms to calculate RUSLE factors of slope length (L) and slope steepness (S) in Switzerland. Geomorphology, 346, p.106850.

Blewitt, G. (1997) 'Basics of the GPS technique: observation equations. Geodetic applications of GPS', 10, p.54.

Boonstra, J. (1994) 'Estimating Peak Runoff Rates', pp. 121–144.

Boyle, D. P., Gupta, H. V. and Sorooshian, S. (2000) 'Toward improved calibration of hydrologic models: Combining the strengths of manual and automatic methods.', Water Resources Research, 36(12), pp. 3663–3674. doi: 10.1029/2000WR900207.

Braca, G. (2008) 'Stage-discharge relationships in open channels: Practices and problems.', London, UK: Univ. degli Studi di Trento, Dipartimento di Ingegneria Civile e Ambientale.

Brakensiek, D. L., Osborn, H. B. and Rawls, W. J. (1979) 'Field manual for research in agricultural hydrology. Agriculture handbook, 224', Journal of Hydrology, 2(3), p. 274. doi: 10.1016/0022-1694(65)90047-8.

C. Alewell, P. Borrelli, K. Meusburger, P. Panagos., (2019) 'Using the USLE: Chances, challenges, and limitations of soil erosion modeling', International Soil and Water Conservation Research, 7(3), pp. 203–225. doi: 10.1016/j.iswcr.2019.05.004.

Caletka, M. et al. (2020) 'Improvement of SCS-CN Initial Abstraction Coe ffi cient in the Czech Republic: A Study of Five Catchments', pp. 1–28.

Chow, V., Maidment, D. and Mays, L. (1988) 'Applied Hydrology.', p. 136.

CNWD (no date) 'Global Positioning System (GPS) Basics', (1), pp. 1–3. Available at: https://www.cityofnewburgh-ny.gov/DocumentCenter/View/1261/Introduction-to-GIS-PDF.

D. Gwapedza, N. Nyamela, D. Hughes, A. Slaughter, S. Mantel, and B.Waal.,(2021) 'Prediction of sediment yield of the Inxu River catchment (South Africa) using the MUSLE', International Soil and Water Conservation Research, 9(1), pp. 37–48. doi: 10.1016/j.iswcr.2020.10.003.

Dabi, N., Fikirie, K. and Mulualem, T. (2017) 'Soil and water conservation practices on crop productivity and its economic implications in Ethiopia: A review'. Asian J. Agric. Res., 11: 128-136.: doi: 10.3923/ajar.2017.128.136.

Davie, T. and Quinn, N. (2019) Fundamentals of Hydrology, Second Edition. Routledge

Desta L., Carucci V., Wendem-Ageliehu A., and Abebe Y., (2005) 'Community-based Participatory Watershed Development: A Guideline', (January 2005).

Desta, G., Klik, A. and Hurni, H. (2009) 'Assessment of soil erosion and soil conservation practices in Angereb watershed, Ethiopia: technological and land user context', (August 2008).

DHV and DELFT (2001) 'Hydrometry Design Manual', Volume 4', 4.

Diplas, P., Kuhnle, R., Gray, J., Glysson, D. and Edwards, T., (2008) 'Sediment Transport Measurements Sedimentation Engineering: Theories, Measurements, Modeling, and Practice'. ASCE Manuals and Reports on Engineering Practice, pp. 305–352.

Djoukbala, O., Hasbaia, M., Benselama, O. and Mazour, M., (2019). Comparison of the erosion prediction models from USLE, MUSLE and RUSLE in a Mediterranean watershed, case of Wadi Gazouana (NW of Algeria). Modeling Earth Systems and Environment, 5(2), pp.725-743.

Donigian, T. and Bicknell, B. (2006) 'Sediment Parameter and Calibration Guidance for HSPF', US Environmental Protection Agency, Office of Water, Washington, DC, (January), p. 43 p.

El-Ashmawy, K. L. (2016) 'Investigation of the accuracy of google earth elevation data'. Artificial Satellites, 51(3), pp.89-97', 51(3). doi: 10.1515/arsa-2016-0008.

ERADM (2013) 'Drainage Design Manual'.

ESRI (2002) 'ArcGIS 9: using ArcGIS Spatial Analyst.'

ESRI (2010) 'Spatial Analyst Tutorial', Available at: https://help.arcgis.com/en/arcgisdesktop/10.0/pdf/spatial-analyst-tutorial.pdf.

Esser, K., Vågen, T. G. and Haile, M. (2002) 'Soil conservation in Tigray.' Soil Conservation, (5), pp. 1–21.

FEPA (2004) 'The Federal Environmental Protection Authority Guidelines on Soil Conservation on Cultivated Land'.

Flanagan, D., Nearing, M. and Norton, L. (2002) 'Soil erosion by water prediction technology developments in the United States. Modeling erosion, sediment transport, and sediment yield', (60).

Garnero, G. and Godone, D. (2013) 'Comparisons between different interpolation techniques', The International Archives of the Photogrammetry, Remote Sensing and Spatial Information Sciences, 5, pp. 27–28. doi: 10.5194/isprsarchives-XL-5-W3-139-2013.

Gelagay, H. S. and Minale, A. S. (2016) 'Soil loss estimation using GIS and Remote sensing techniques: A case of Koga watershed, Northwestern Ethiopia', International Soil and Water Conservation Research, 4(2), pp. 126–136. doi: 10.1016/j.iswcr.2016.01.002.

Girmay, G., Moges, A. and Muluneh, A. (2020) 'Estimation of soil loss rate using the USLE model for Agewmariayam Watershed, northern Ethiopia', Agriculture and Food Security, 9(1), pp. 1–12. doi: 10.1186/s40066-020-00262-w.

Gomez, K. A., and Gomez, A. A. (1984) 'Statistical procedures for agricultural research.', John Wiley & sons, 6.

Gray, J. R., Simões, F. J. M. and Introduction, D. (2008) 'Estimating Sediment Discharge', pp. 1065–1086.

Grunder, M., 1988. Soil conservation research in Ethiopia. Mountain research and development, pp.145-151.

Guzman, C.D., Tilahun, S.A., Zegeye, A.D. and Steenhuis, T.S., 2013. Suspended sediment concentration–discharge relationships in the (sub-) humid Ethiopian highlands. Hydrology and Earth System Sciences, 17(3), pp.1067-1077.

Haithcoat, T. (1999) 'Spatial Interpolation'.

Held, A, Phinn S, Soto-Berelov M, Jones S, (2015) 'AusCover good practice guidelines. A technical handbook supporting calibration and validation activities of remotely sensed data products. Chapter 6. Calibration and Validation.'

Hickin (2004) 'River Geomorphology, Chapter 4 Sediment Transport.'.

Hörmann, G., Zhang, X. and Fohrer, N. (2007) 'Comparison of a simple and a spatially distributed hydrologic model for the simulation of a lowland catchment in Northern Germany', Ecological Modelling, 209(1), pp. 21–28. doi: 10.1016/j.ecolmodel.2007.07.019.

Hrabalikova, M. and Janeček, M., 2017. Comparison of different approaches to LS factor calculations based on a measured soil loss under simulated rainfall. Soil and water research, 12(2), pp.69-77.

Hu, Q., Wu, W., Xia, T., Yu, Q., Yang, P., Li, Z. and Song, Q., (2013) 'Exploring the Use of Google Earth Imagery and Object-Based Methods in Land Use/Cover Mapping', pp. 6026–6042. doi: 10.3390/rs5116026.

Humberto, B. and Rattan, L. (2008) Principles of Soil Conservation and Management. (Vol. 167169). New York: Springer.

Hurni, H. (1985) 'Erosion-productivity-conservation systems in Ethiopia, (January 1985).

Hurni, H., Abate, S., Bantider, A., Debele, B., Ludi, E., Portner, B., Yitaferu, B. and Zeleke, G., (2010) 'Land Degradation and Sustainable Land Management in the Highlands of Ethiopia', Global Change and Sustainable Development, 9(6), pp. 529–542. doi: 10.1002/(SICI)1099-145X (199811/12)9:6<529: AID-LDR313>3.0.CO;2-O.

Hurni, H., Berhe, W.A., Chadhokar, P., Daniel, D., Gete, Z., Grunder, M. and Kassaye, G., (2016) 'Soil and Water Conservation in Ethiopia: Guidelines for Development Agents.' Second revised edition.

IDNR (2009) 'Iowa Storm Water Management Manual', Iowa Department of Natural Resources, (Lid).

Isioye, O. A., Jobin, P. and Youngu, T. T. (2012) 'An assessment of digital elevation models (DEMs) from different spatial data sources.'

J. G. Arnold, D. N. Moriasi, P. W. Gassman, K. C. Abbaspour, M. J. White, R. Srinivasan, C. Santhi, R. D. Harmel, A. van Griensven, M. W. Van Liew, N. Kannan, M. K. Jha, (2012), SWAT: model use, calibration, and validation.

J. Vrugt, H. Gupta, L. Bastidas, W. Bouten, and S. Sorooshian., (2003) 'Effective and efficient algorithm for multiobjective optimization of hydrologic models', 39(8), pp. 1–19. doi: 10.1029/2002WR001746.

Jackson, W.L., Gebhardt, K. and Van Haveren, B.P., (1986). Use of the modified universal soil loss equation for average annual sediment yield estimates on small rangeland drainage basins. IAHS-AISH publication, (159), pp.413-423.

Jetten, V. and Maneta, M. (2011) 'Calibration of Erosion Models, Handbook of Erosion Modelling'.

John Doherty (2004) '"PEST" Model-Independent Parameter Estimation User Manual': 5th Edition'.

K.G. Renard, G.R Foster, G.A. Weesies, D.K. McCool, and D.C. Yoder., (2000) Predicting Soil Erosion by Water: A Guide to Conservation Planning with the Revised Universal Soil Loss Equation (RUSLE).

Kent, K.M., Woodward, D.E. and Hoeft, C.C., (2010) 'National Engineering Handbook Chapter 15 Time of Concentration'.

Kitsikoudis, V., Sidiropoulos, E. and Hrissanthou, V. (2013) 'Derivation of sediment transport models for sand-bed rivers from data-driven techniques. Sediment Transport Processes and Their Modelling Applications.', (1942). Available at: http://dx.doi.org/10.5772/53432.

Kulkarni, M. N. (2003) 'The Global Positioning System and Its Applications.'.

Kuzmin, V., Seo, D.-J. and Koren, V. (2008) 'Fast and efficient optimization of hydrologic model parameters using a priori estimates and stepwise line search', pp. 109–128. doi: 10.1016/j.jhydrol.2008.02.001.

Lachow, I. (1995) 'The GPS Dilemma: Balancing Military Risks and Economic Benefits.' Author (s): Irving Lachow Published by: The MIT Press the GPS Dilemma Irving Lachow', 20(1), pp. 126–148.

Legates, D. R. and McCabe, G. J. (1999) 'Evaluating the use of "goodness-of-fit" measures in hydrologic and hydroclimatic model validation.', Water Resources Research, 35(1), pp. 233–241. doi: 10.1029/1998WR900018.

M. Bos, R. Kselik, R. Allen, and D. Molden, (2008) 'Water Requirements for Irrigation and the Environment. Springer.

Mccuen, R. H., Johnson, P. A. and Ragan, R. M. (2002) 'Highway Hydrology', (2).

McGowen, P. and McNally, M. (2007) 'Evaluating the Potential to Predict Activity Types from GPS and GIS Data'. In Transportation Research Board 86th Annual Meeting.

Mei, G., Tipper, J. C. and Xu, N. (2012) 'Discrete Surface Modeling Based on Google Earth: A Case Study.', In Proceedings of 2012 2nd International Conference on Computer Science and Network Technology.

Mekonen, K. and Tesfahunegn, G.B., (2011). Impact assessment of soil and water conservation measures at Medego watershed in Tigray, northern Ethiopia. Maejo International Journal of Science and Technology, 5(3), p.312.

Mishra, S. and Singh, V. (2003) 'SCS-CN Method. In Soil conservation service curve number (SCS-CN) methodology.' (pp. 84-146). Springer, Dordrecht.'

Mishra, S.K., Pandey, A. and Singh, V.P., (2015). Special issue on soil erosion and sediment yield modeling. Journal of Hydrologic Engineering, 20(6), p.C2015001.

Mohammed, S. (2017) 'Working with Google Earth Pro to Prepare Land Use Land Cover Maps and Own digital elevation Model (DEM)'.

Moriasi, D. N. et al. (2007) 'Model Evaluation Guidelines for Systematic Quantification of Accuracy In Watershed Simulations', 50(3), pp. 885–900.

Moriasi, D.N., Gitau, M.W., Pai, N. and Daggupati, P., (2015). Hydrologic and water quality models: Performance measures and evaluation criteria. Transactions of the ASABE, 58(6), pp.1763-1785.

MSF-OCA (no date) 'Guide to Global Position Systems (GPS)', pp. 1–9. Available at: https://evaluation.msf.org/sites/evaluation/files/guide_to_global_position_systems.pdf.

Muche, H., Temesgen, M. and Yimer, F. (2013) 'Soil loss prediction using USLE and MUSLE under conservation tillage integrated with "Fanya jus" in', 3(10), pp. 46–52.

Najib, S., Aliah, S. and Hamidon, H. (2020) 'Suspended Sediment Concentration and Sediment Loading of Bernam River (Perak, Malaysia).', Transylvanian Review of Systematical and Ecological Research, 2, pp. 1–14. doi: 10.2478/trser-2020-0007.

Namirembe, S., Nzyoka, J. M. and Gathenya, J. M. (2015) 'A guide for selecting the right soil and water conservation practices for smallholder farming in Africa.'

Ndomba, P., Mtalo, F. and Killingtveit, A., (2008). SWAT model application in a data scarce tropical complex catchment in Tanzania. Physics and Chemistry of the Earth, Parts A/B/C, 33(8-13), pp.626-632.

Nearing, M. A. (2011) 'Model Development: A User' s Perspective'.

NMA, (2019), Ethiopian national meteorology agency.

NRCS (2004) 'Part 630 Hydrology National Engineering Handbook Chapter 10 Estimation of Direct Runoff from Storm Rainfall'.

Panagos, P., Borrelli, P. and Meusburger, K. (2015) 'A new European slope length and steepness factor (LS-factor) for modeling soil erosion by water.', Geosciences (Switzerland), 5(2), pp. 117–126. doi: 10.3390/geosciences5020117.

Pandey, S., Kumar, P., Zlatic, M., Nautiyal, R. and Panwar, V.P., (2021) 'International Soil and Water Conservation Research Recent advances in the assessment of soil erosion vulnerability in a watershed', 9.

Pegram, G. G. S., and Sinclair, D. S. (2002) 'A linear catchment model for real-time flood forecasting.', Water Research Commission., (1005).

Qian, G. and Mahdi, A. (2020) 'Sensitivity analysis methods in the biomedical sciences.', Mathematical biosciences. 323, p.108306.

R. Cronshey, R. McCuen, MD. Park, N. Miller, W. Rawls, MD. Beltsville, and S. Robbins., (1986) 'Urban Hydrology for Small Watersheds TR-55', USDA Natural Resource Conservation Service, p. 164. doi: Technical Release 55.

R.By, R. Knippers, Y. Sun, M. Ellis, M. Kraak, M.Weir, Y. Georgiadou, M. Radwan, Cees. Westen, W. and Kainz, E.Sides., (2001) 'Principles of Geographic Information System'. ITC Educational Textbook Series, ITC, Enscheda, The Netherlands.

Ramírez, J. A. (2000) 'Prediction and Modeling of Flood Hydrology and Hydraulics. Chapter 11 of Inland Flood Hazards: Human, Riparian and Aquatic Communities Eds.', Ellen Wohl; Cambridge University Press., pp. 1–52.

Randle, T., Yang, T. and Joseph, D. (2006) 'Erosion and Reservoir Sedimentation, Erosion and Sedimentation Manual', (November).

Raza, A., Ahrends, H., Habib-Ur-Rahman, M. and Gaiser, T., (2021). Modeling approaches to assess soil erosion by water at the field scale with special emphasis on heterogeneity of soils and crops. Land, 10(4), p.422.

Reddy, K.S., Kumar, R.N., Rao, K.V., Maruthi, V., Reddy, B.M.K. and Venkateswarlu, B., (2012) 'User Manual for Surface Water Yield Model (SWYMOD).'

Renard, K. G., G. R. Foster, G. A. Weesies, D. K. McCool, and D. C. Yoder., (1997) 'Predicting Soil Erosion by Water: A Guide to Conservation Planning with the Revised Universal Soil Loss Equation.', 2(March).

Roose, E. (1996) 'Land husbandry - Components and strategy,' by Director of Soils Research. Rome: FAO

Rusli, N., Majid, M. R. and Din, A. H. M. (2014) 'Google Earth's derived digital elevation model: A comparative assessment with Aster and SRTM data.'. doi: 10.1088/1755-1315/18/1/012065.

Sadeghi, S., Mizuyama, T. and Ghaderi, V. (2007) 'Conformity of MUSLE estimates and erosion plot data for storm-wise sediment yield estimation', Terrestrial, Atmospheric and Oceanic Sciences, 18(1), pp. 117–128. doi: 10.3319/TAO.2007.18.1.117(O).

Satheeshkumar, S., Venkateswaran, S. and Kannan, R. (2017) 'Rainfall – runoff estimation using SCS – CN and GIS approach in the Pappiredipatti watershed of the Vaniyar sub basin, South India', Modeling Earth Systems and Environment, 3(1), pp. 1–8. doi: 10.1007/s40808-017-0301-4.

Schmidt, J. (2000) 'Soil Erosion: Application of physically-based models.'.

SDTG (2002) 'Soil Erodibility (K) Factors and Soil Loss Tolerance (T) Factor', (August), p. 2002.

Sharpley, A. N., and Williams, J. R. (1990) 'EPIC: The erosion-productivity impact calculator', U.S. Department of Agriculture Technical Bulletin, (1768), p. 235. Available at: http://agris.fao.org/agris-search/search.do?recordID=US9403696.

Shilton, P., Norman, P., Stone, B. and Carey, B., (2015) 'Soil conservation guidelines for Queensland. Peak discharge estimation', Department of Science, Information Technology and Innovation., pp. 1–19.

Shin, G., (1999).'The Analysis of Soil Erosion Analysis in Watershed using GIS.' Ph. D. Thesis, Department of Civil Engineering, Gang-won National University, Gangwon-do, Korea,

Smith, S.J., Williams, J.R., Menzel, R.G. and Coleman, G.A., (1984) 'Prediction of Sediment Yield from Southern Plains Grasslands with the Modified Universa1 Soil Loss Equation.', 37(July), pp. 295–297., Rangeland Ecology & Management/Journal of Range Management Archives.

Sprenger, F.D., (1978). 'Determination of direct runoff with the curve number method in the coastal area of Tanzania/East Africa.' Wasser Boden, 1.

Stauffer, M. T. (2018) 'Introductory: Chapter: The Many Faces of Calibration and Validation in Analytical Methodology in the Present Day.', pp. 3–14. doi: 10.5772/intechopen.75304.

Stone, J.J., Lane, L.J., Shirley, E.D. and Renard, K.G., (1986). Runoff-Sediment Yield Model for Semiarid Regions. In Proceedings of the Fourth Federal Interagency Sedimentation Conference March 24-27, 1986, Las Vegas, Nevada. (Vol. 2).

Subramanya, K. (2013) 'Engineering Hydrology,' 4e. Tata McGraw-Hill Education. Third.

Tatiana, M. and José, M. (2021) 'Comparison of statistical indices for the evaluation of crop models performance', pp. 9675–9684. Available at: https://doi.org/10.15446/rfnam.v74n3.93562 Tatiana.

Taylor, M. A., Woolley, J. E. and Zito, R. (2000) 'Integration of the global positioning system and geographical information systems for traffic congestion studies.'. Transportation Research Part C: Emerging Technologies, 8(1-6), pp.257-285.

Tilrem, O. A. (1979) 'Manual on Procedures in Operational Hydrology Volume 3 Stream Discharge Measurements by Current Meter and Relative Salt Dilution', 3 Ministry of Water Energy and Minerals Tanzania, Norwegian Agency for International Development (NORAD).

Tollner, E.W., (2016). Engineering hydrology for natural resources engineers.' John Wiley & Sons.

Tsige, M.G., Malcherek, A. and Seleshi, Y., (2022). Estimating the Best Exponent of the Modified Universal Soil Loss Equation and Regionalizing the Modified Universal Soil Loss Equation Under Hydro-climatic Condition of Ethiopia.

Turnipseed, D. P., and Sauer, V. B. (2010) 'Discharge measurements at gaging stations', Techniques of Water-Resources Investigations of the United States Geological Survey. Book 3 - p. 171. Available at: https://pubs.usgs.gov/twri/twri3a8/pdf/TWRI_3-A8.pdf.

USDA (2019) 'Title 430 – National Soil Survey Handbook Part 618 – Soil Properties and Qualities Subpart A – General Information', (August), pp. 1–97.

USDA. (2009) 'Soil Quality Indicators, Total Organic Carbon'. Natural Resources Conservation Service., http://soils. usda. gov/sqi/assessment/files/toc_sq_biological_indicator_sheet. pdf.

Valentina, K. and Frank, W. (2000) ‘SWIM (Soil and Water Integrated Model) User Manual 2. Mathematical Description of the Model Components’, Potsdam Institute for Climate Impact Research, Potsdam, Germany in collaboration with Jeff Arnold, Ragavan Srinivasan, and Jimmy Williams USDA ARS, Temple, TX, USA.

Vaze, J., Jordan, P., Beecham, R., Frost, A., and Summerell, G., (2011) 'Guidelines for Rainfall-Runoff Modelling: Towards Best Practice Model Application'. Australia: eWater Cooperative Research Centre.

Westenbroek, S. M. et al. (2018) ‘SWB Version 2. 0 — A Soil-Water-Balance Code for Estimating Net Infiltration and Other Water-Budget Components’.

Williams, J. R., and Berndt, H. D. (1977) ‘Sediment Yield Prediction Based on Watershed Hydrology.’, Transactions of the American Society of Agricultural Engineers, 20(6), pp. 1100–1104. doi: 10.13031/2013.35710.

Wischmeier, W. H. and Smith, D. D. (1978) ‘Predicting rainfall erosion losses a guide to conservation planning (No. 537).’, Agriculture handbook no. 537, (537), pp. 285–291. Department of Agriculture, Science, and Education Administration.

WMO (1994) ‘Guide to hydrological practices. WMO-168. Data acquisition and processing, analysis, forecasting, and other applications data acquisition and processing,' Fifth edition, WMO-No. 168’.

WMO (2010) 'Manual on Stream Gauging'. WMO-No. 1044

Wu, W. (2019) ‘Lecture 9 Spatial Interpolation’, pp. 1–19.

Xiaoqing, Y. (2003) 'manual On Sediment Management and Measurement", World Meteorological Organization Operational Hydrology Report No. 47, WMO-No. 948.

Yang, C.S., Kao, S.P., Lee, F.B. and Hung, P.S., (2004) ‘Twelve different interpolation methods: A case study of Surfer 8.0'. In Proceedings of the XXth ISPRS Congress (Vol. 35, pp. 778-785).

Yapo, P. O., Gupta, H. V. and Soroosh, S. (1997) ‘multi-objective global optimization for hydrologic models, the university of Arizona’.

Yesuf, M., Mekonnen, A., Kassie, M. and Pender, J., (2005) ‘Cost of land degradation in Ethiopia: A critical review of past studies.'. Addis Ababa, Ethiopia: EDRI/EEPFE.

Z.Y. Shen *, Y.W. Gong, Y.H. Li, Q. Hong, L. Xu, R.M. Liu, (2009) ‘A comparison of WEPP and SWAT for modeling soil erosion of the Zhangjiachong Watershed in the Three Gorges Reservoir Area’, 96, pp. 1435–1442. doi: 10.1016/j.agwat.2009.04.017.

Appendix

Appendix table 1 Curve Number for Hydrological Soil Cover Complexes for Antecedent Soil Moisture Condition Class II and Ia= 0.2S

Cover description		Curve numbers for hydrologic soil group				
Cover type	**Treatment**	**Hydrologic condition**	**A**	**B**	**C**	**D**
Fallow	Bare soil		77	86	91	94
	Crop residue cover (CR)	Poor	76	85	90	93
		Good	74	83	88	90
Row crops	Straight row (SR)	Poor	72	81	88	91
		Good	67	78	85	89
	Straight row (SR) + Crop residue cover	Poor	71	80	87	90
		Good	64	75	82	85
	Contoured (C)	Poor	70	79	84	88
		Good	65	75	82	86
	Contoured (C) + Crop residue cover (CR)	Poor	69	78	83	87
		Good	64	74	81	85
	Contoured & terraced (C&T)	Poor	66	74	80	82
		Good	62	71	78	81
	Contoured & terraced (C&T) + Crop residue cover (CR)	Poor	65	73	79	81
		Good	61	70	77	80
Small grain	Straight row (SR)	Poor	65	76	84	88
		Good	63	75	83	87
	Straight row (SR) + Crop residue cover	Poor	64	75	83	86
		Good	60	72	80	84
	Contoured (C)	Poor	63	74	82	85
		Good	61	73	81	84
	Contoured (C) + Crop residue cover (CR)	Poor	62	73	81	84
		Good	60	72	80	83
	Contoured & terraced (C&T)	Poor	61	72	79	82
		Good	59	70	78	81
	Contoured & terraced (C&T) + Crop residue cover (CR)	Poor	60	71	78	81
		Good	58	69	77	80
Closs Seeded or broadcast legumes or rotation meadow	Straight row (SR)	Poor	66	77	85	89
		Good	58	72	81	85
	Contoured (C)	Poor	64	75	83	85
		Good	55	69	78	83
	Contoured & terraced (C&T)	Poor	63	73	80	83
		Good	51	67	76	80

Source:(Cronshey *et al.*, 1986).

Appendix table 2 Runoff Curve Number for Other Agricultural Lands

Cover description	Curve numbers for hydrologic soil group				
Treatment	Hydrologic condition	A	B	C	D
Pasture, grassland, or range—continuous forage for grazing	Poor	68	79	86	89
	Fair	49	69	79	84
	Good	39	61	74	80
Meadow—continuous grass, protected from grazing and generally mowed for hay.		30	58	71	78
Brush—brush-weed-grass mixture with a brush is the major element.	Poor	48	67	77	83
	Fair	35	56	70	77
	Good	30	48	65	73
Woods—grass combination (orchard or tree farm).	Poor	57	73	82	86
	Fair	43	65	76	82
	Good	32	58	72	79
Woods.	Poor	45	66	77	83
	Fair	36	60	73	79
	Good	30	55	70	77
Farmsteads—buildings, lanes, driveways, and surrounding lots.		59	74	82	86

Source: (Cronshey *et al.*, 1986).

Appendix table 3 Soil hydrological group (SHG)

Soil Texture	Hydrologic Soil Group
Sand, Loamy sand, Sandy loam	A
Silt loam or Loam	B
Sandy clay loam,	C
Clay loam, Silty clay loam, sandy clay, Silty clay, or Clay	D

Source: (Cronshey *et al.*, 1986).

Appendix table 4 Regression coefficients for SCS graphical peak discharge method for the type II rainfall distribution recommended for Ethiopia (ERADM, 2013).

Ia/P	C0	C1	C2
0.10	2.55323	-0.61512	-0.16403
0.30	2.46532	-0.62257	-0.11657
0.35	2.41896	-0.61594	-0.0882
0.40	2.36409	-0.59857	-0.05621
0.45	2.29238	-0.57005	-0.02281
0.50	2.20282	-0.51599	-0.01259

Source: (Cronshey *et al.*, 1986).

Appendix figure 1 Velocity Vs. Slope Graph for Shallow concentrated Flow

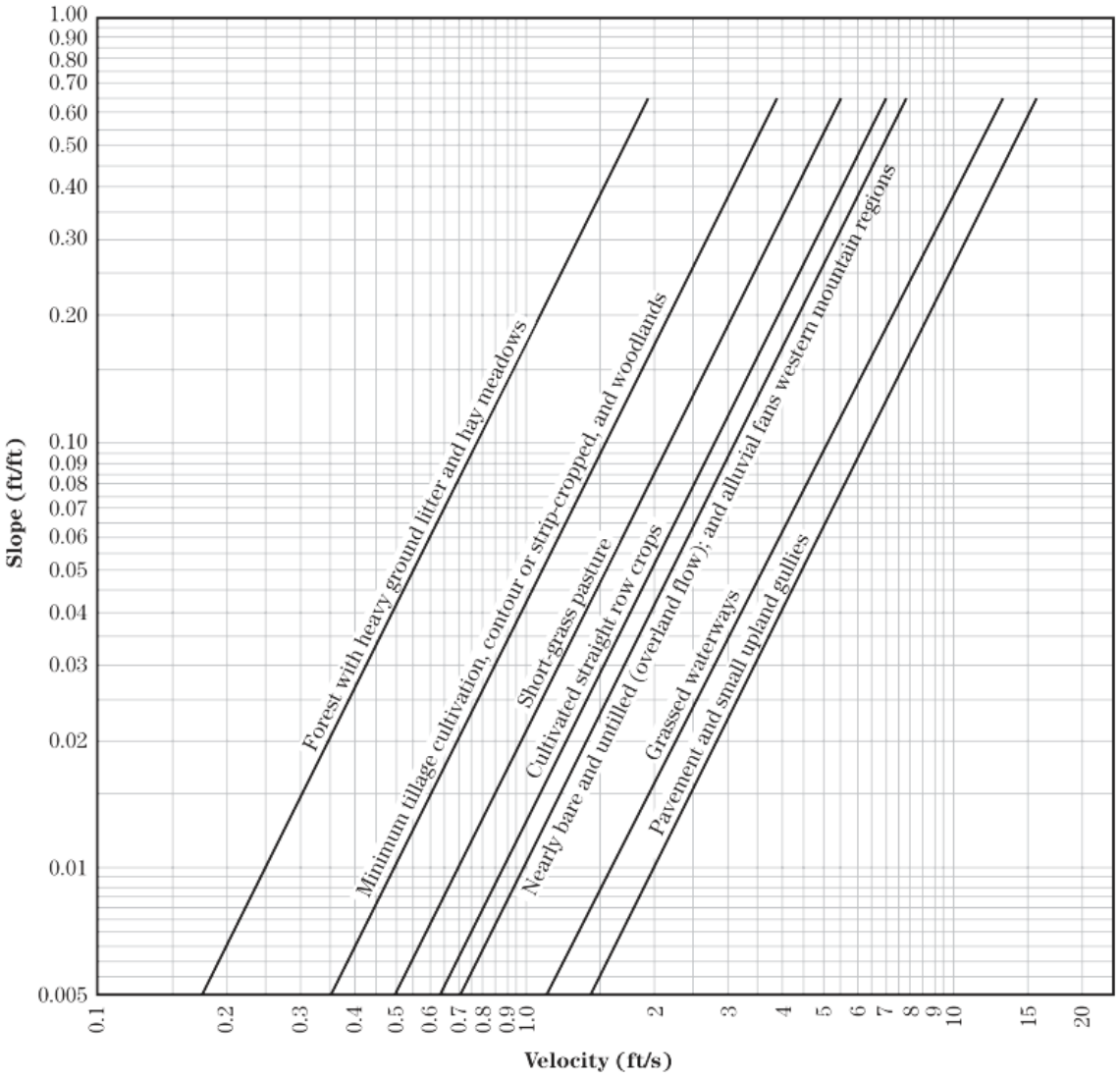

Source: (Kent *et al.*, 2010).

Appendix table 5 Manning's Roughness Coefficients for Sheet Flow

Surface description		n
Smooth surface	concrete, asphalt, gravel, or bare soil	0.011
	Fallow (no residue)	0.05
Cultivated soils:	Residue cover ≤ 20%	0.06
	Residue cover > 20%	0.17
Grass:	Short-grass prairie	0.15
	Dense grasses	0.24
	Bermudagrass	0.41
	Range (natural)	0.13
Woods	Light underbrush	0.40
	Dense underbrush	0.80

Source: (Kent *et al.*, 2010)

Appendix table 6 Manning's Roughness Coefficients for Open Channel Flow

Material		Typical Manning roughness coefficient
Concrete		0.012
Gravel bottom with sides	Concrete	0.020
	Mortared stone	0.023
	Riprap	0.033
Natural stream channels		
Clean Straight stream		0.035
Clean winding stream		0.040
Winding with weeds and pools		0.050
With heavy brush and limber		0.100
Flood Plains		
Pasture		0.035
Field crops		0.040
Light bush and weeds		0.050
Dense brush		0.070
Dense trees		0.100

Source: (Chow *et al.*, 1988)

Appendix table 7 Value of M in the Calculation of LS Factor.

Slope Range	M Value
< 1	0.2
1-3	0.3
3.5-4.5	0.4
> 5	0.5

Source: (Wischmeier and Smith, 1978).

Appendix table 8 Cover management factor (C) value adopted from different sources

Land use	C-value	Reference
Settlement	0.15	(Hurni, 1985)
Cultivated Land	0.15	(Hurni, 1985), (Girmay *et al.*, 2020)
Ethiopian teff	0.25	(Hurni, 1985)
sorghum	0.1	(Hurni, 1985)
Cereals	0.15	(Hurni, 1985)
Pulses	0.15	(Hurni, 1985)
Linseed	0.25	Panagos (2015)
Bushland	0.012	(Wischmeier and Smith, 1978)
Scattered bushland	0.14	(Wischmeier and Smith, 1978)
Bare land	1	Hurni, 1985), (Wischmeier and Smith, 1978)

Appendix table 9 Support practice factor (P) value adopted from different sources

Slope %	Contouring	Strip Cropping	Terracing
0.0 -7.0	0.55	0.27	0.10
7.0 – 11.3	0.6	0.30	0.12
11.3 - 17.6	0.8	0.40	0.16
17.6 – 26.8	0.9	0.45	0.18
> 26.8	1.0	0.50	0.20

Source: (Shin, 1999).

Appendix table 10 Evaluation Ratings for watershed-scale models

Table 8. Initial performance evaluation criteria for recommended statistical performance measures for watershed- and field-scale models based on the distribution of existing data.

Measure	Component	Temporal Scale	*n*	Very Good	Good	Satisfactory	Not Satisfactory
Watershed scale							
R^2	Flow	Annual	84	>0.75	$0.70 \le R^2 \le 0.75$	$0.60 < R^2 < 0.70$	≤0.60
		Monthly	87	>0.85	$0.80 \le R^2 \le 0.85$	$0.70 < R^2 < 0.80$	≤0.70
		Daily	27	>0.85	$0.70 \le R^2 \le 0.85$	$0.50 < R^2 < 0.70$	≤0.50
	Sediment	Annual	3	-	-	-	-
		Monthly	46	>0.80	$0.65 \le R^2 \le 0.80$	$0.40 < R^2 < 0.65$	≤0.40
		Daily	0	-	-	-	-
	N	Annual	2	-	-	-	-
		Monthly	31	>0.70	$0.60 \le R^2 \le 0.70$	$0.30 < R^2 < 0.60$	≤0.30
		Daily	0	-	-	-	-
	P	Annual	0	-	-	-	-
		Monthly	31	>0.80	$0.65 \le R^2 \le 0.80$	$0.40 < R^2 < 0.65$	≤0.40
		Daily	0	-	-	-	-
	General		311	>0.80	$0.70 \le R^2 \le 0.80$	$0.50 < R^2 < 0.70$	≤0.50
NSE	Flow	Annual	71	>0.75	$0.60 \le NSE \le 0.75$	$0.50 < NSE < 0.60$	≤0.50
		Monthly	109	>0.85	$0.70 \le NSE \le 0.85$	$0.55 < NSE < 0.70$	≤0.55
		Daily	79	>0.80	$0.70 \le NSE \le 0.80$	$0.50 < NSE < 0.70$	≤0.50
	Sediment	Annual	4	-	-	-	-
		Monthly	31	>0.80	$0.70 \le NSE \le 0.80$	$0.45 < NSE < 0.70$	≤0.45
		Daily	3	-	-	-	-
	N	Annual	0	-	-	-	-
		Monthly	31	>0.70	$0.60 \le NSE \le 0.70$	$0.35 < NSE < 0.60$	≤0.35
		Daily	6	>0.55	$0.40 \le NSE \le 0.55$	$0.25 < NSE < 0.40$	≤0.25
	P	Annual	10	>0.65	$0.60 \le NSE \le 0.65$	$0.50 < NSE < 0.60$	≤0.50
		Monthly	33	>0.65	$0.50 \le NSE \le 0.65$	$0.40 < NSE < 0.50$	≤0.40
		Daily	1	-	-	-	-
	General		378	>0.80	$0.60 \le NSE \le 0.80$	$0.50 < NSE < 0.60$	≤0.50

Source:(Moriasi *et al.*, 2007)